
ESRF
The European Synchrotron

X-ray imaging

Alexander Rack
European Synchrotron Radiation Facility, Grenoble, France

https://twitter.com/SoM_esrf

WHITE BEAM PHASE CONTRAST RADIOGRAPHY

5 µm resolution, 5 FPS

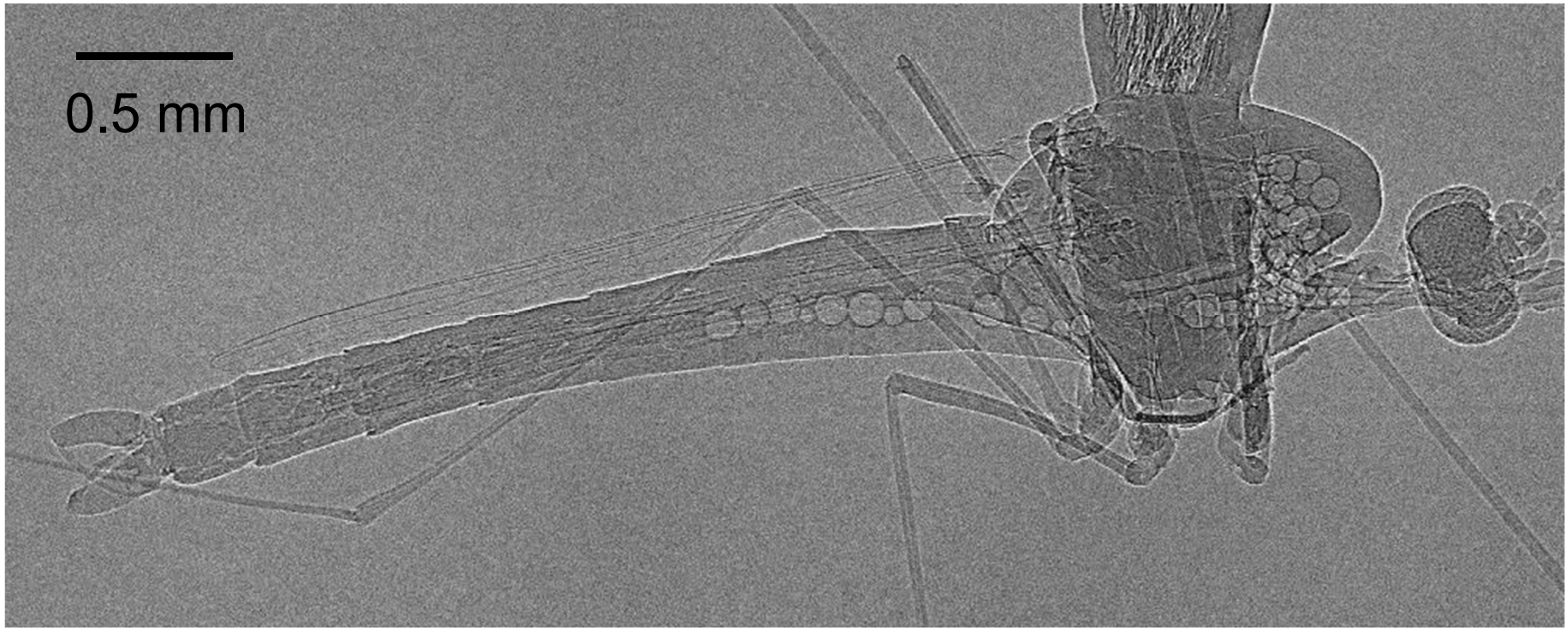

D. Wegrzynek, E. Chinea Cano, C. Streli, P. Wobrauschek, T. Weitkamp, A. Rack, A. Cecilia - ANKA Highlights 2006

FULL-FIELD X-RAY IMAGING – X-RAY IMAGE DETECTORS

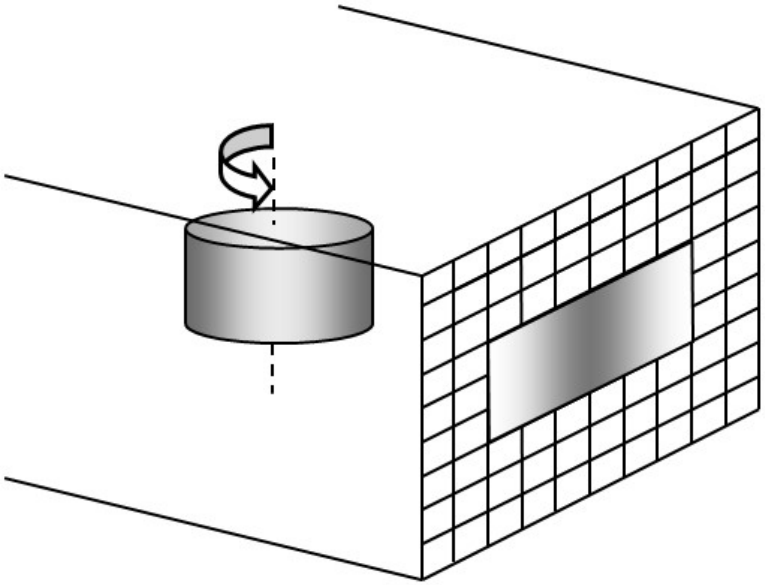

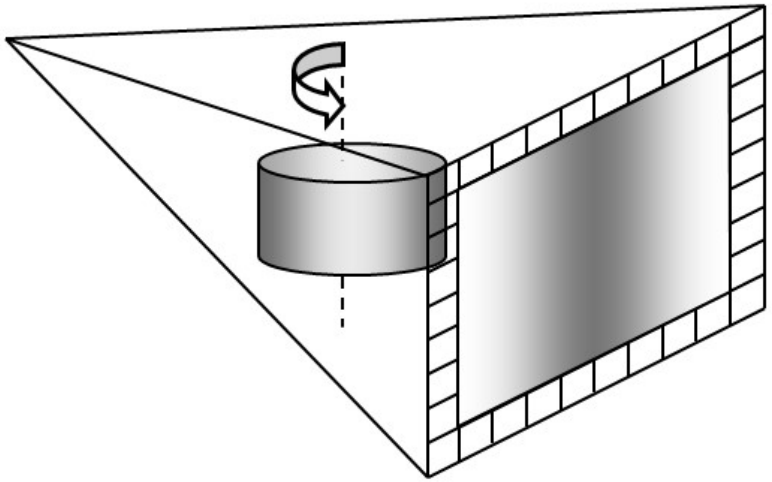

Computed Tomography (CT or CAT)

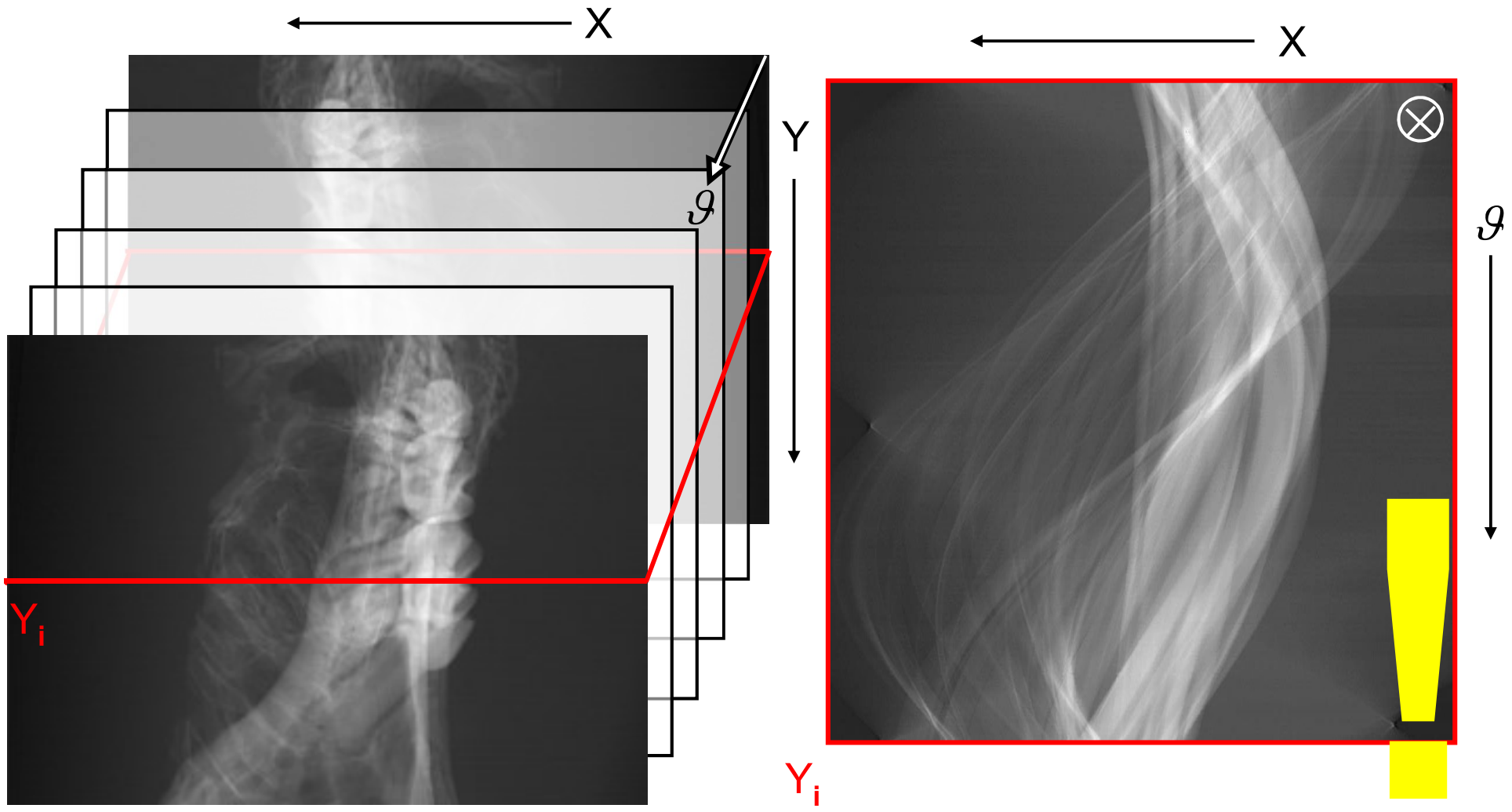

(FILTERED) BACKPROJECTION

$$\frac{\text{number of projections}}{\text{pixels per line}} \geq \frac{\pi}{2}$$

(Shannon's theorem)

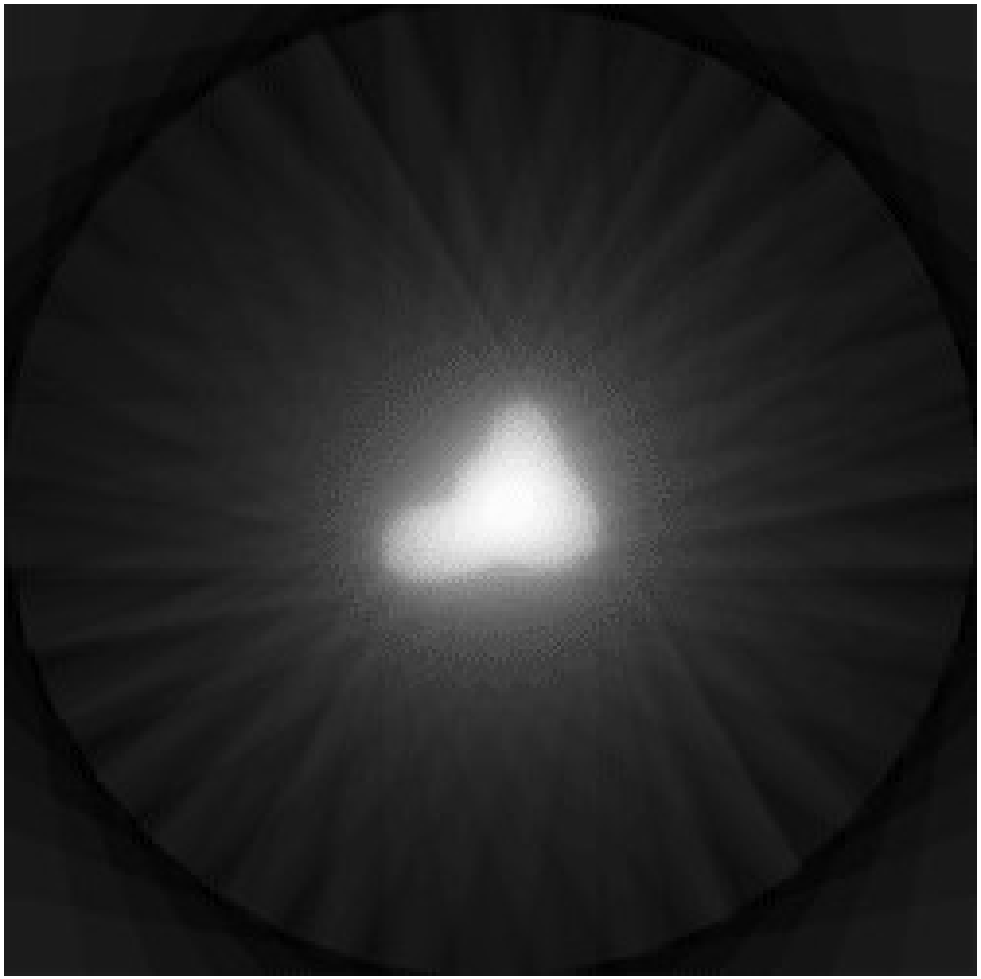

Tomographic Reconstruction

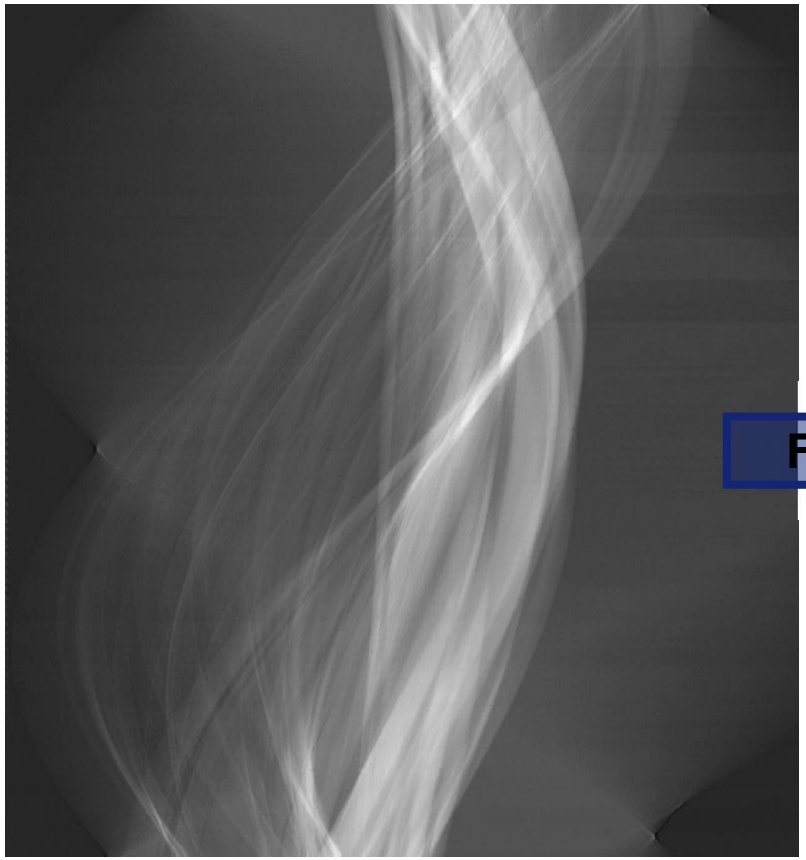

FBP

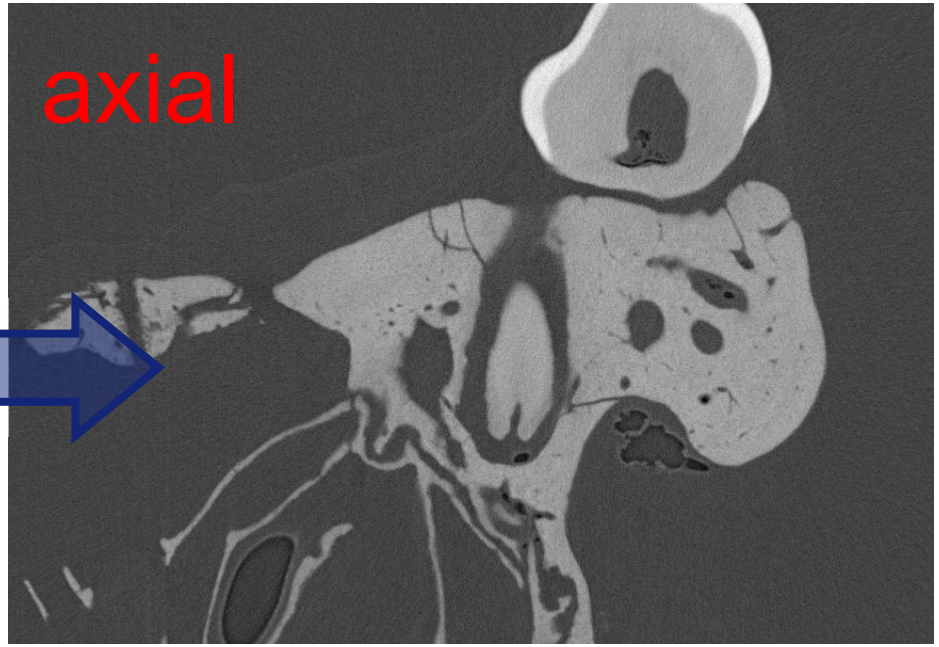

CT – “volume images”

CT: Contrast – Attenuation coefficient

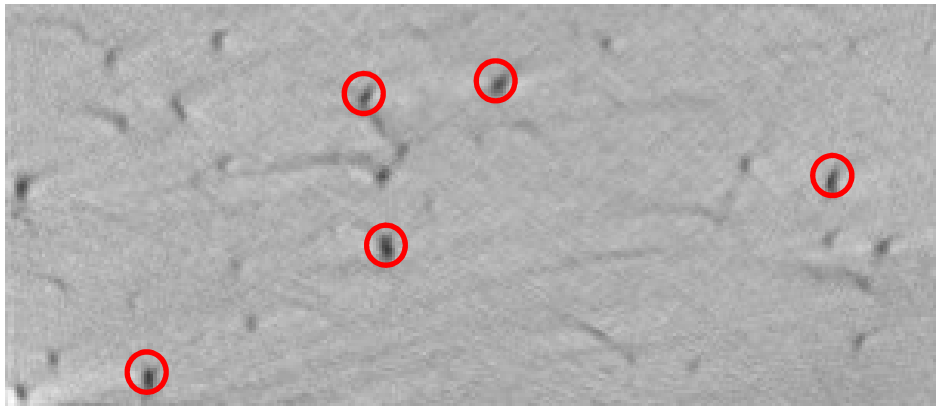

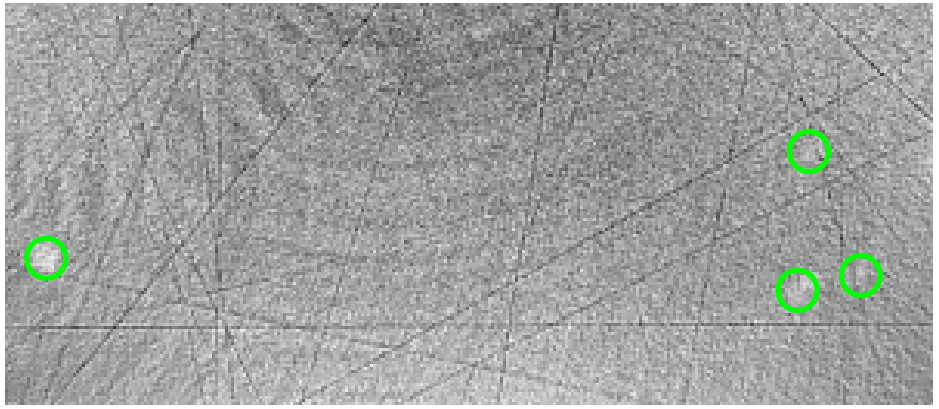

$Zn+TiH_2$
bulk

precursor:

0.50 vol%

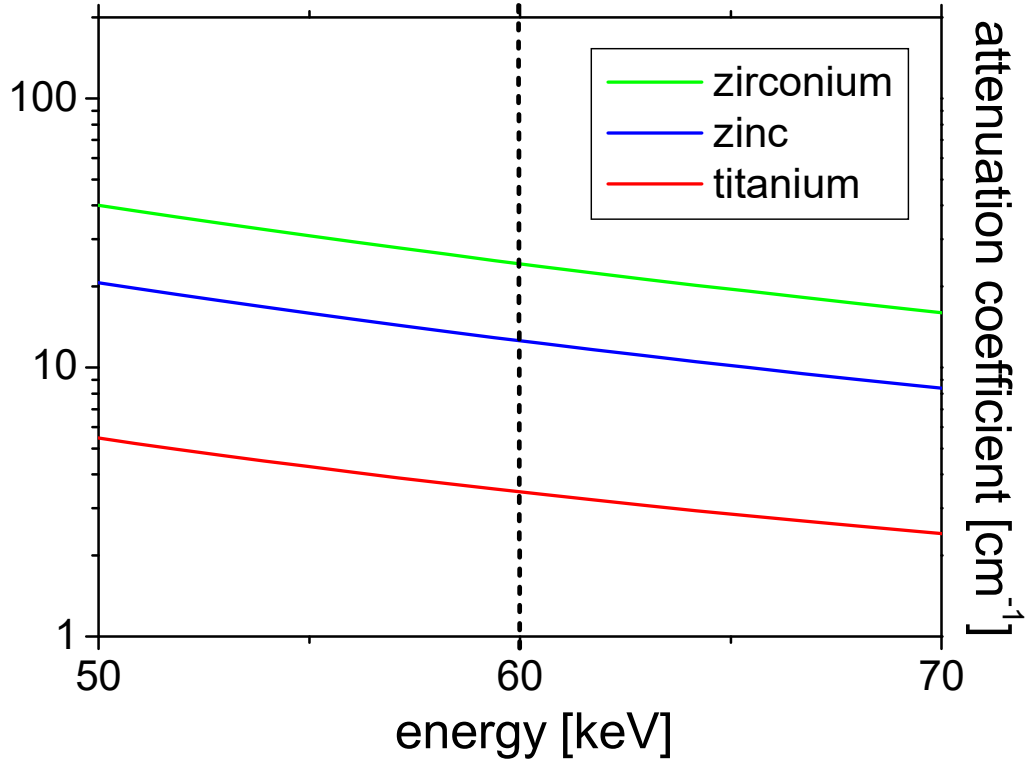

$Zn+ZrH_2$
bulk

precursor:

0.66 vol%

More about X-ray Contrast

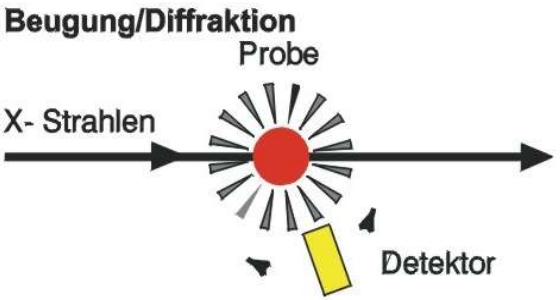

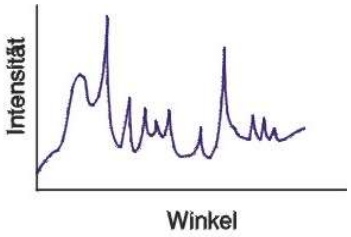

→ Geometric structure on atomic and molecular length scales

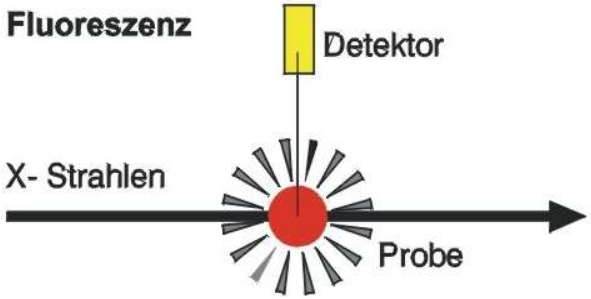

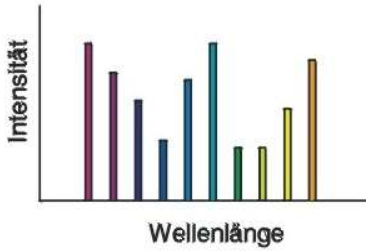

→ Trace element distribution

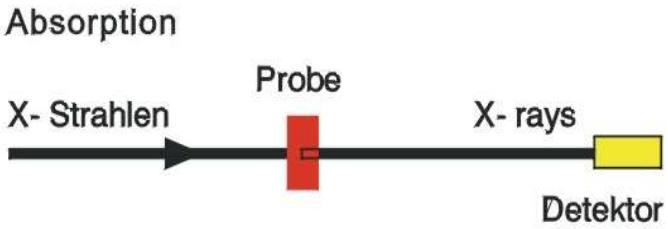

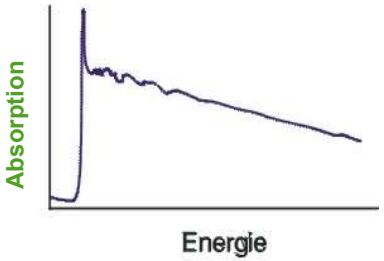

→ Chemical compositio
- Abundant elements,
- their oxidation states
- Geometric structure

on atomic length scales

BRAGG-DIFFRACTION IMAGING / X-RAY TOPOGRAPHY

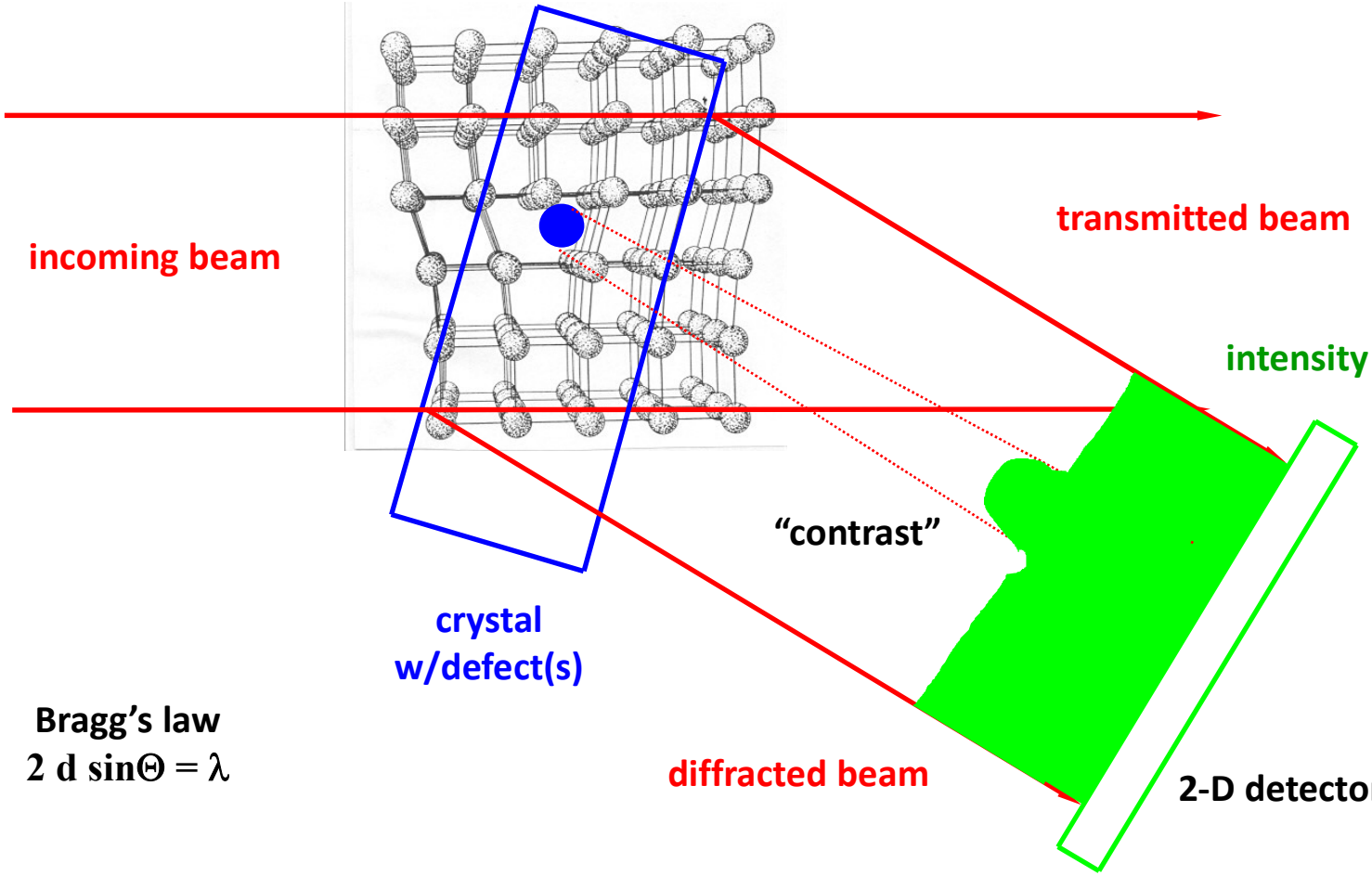

courtesy: J. Härtwig (ESRF)

The Quest for the ideal X-ray Detector

energy-dispersive	scanning	2D/3D XRF, XAS	*silicon drift diode*
high resolution full-field	full-field	magnified (holo-)µCT	*indirect detection*
single photon counting	scanning	ptychography	*pixel detector vs. integrating*
very large field of view	scanning / full-field	2D/3D XRD	*CCD w/taper*

dynamic range, efficiency, noise, read-out, radiation hardness ...

Detector: Micrometer Resolution

Bonse, Busch 1996

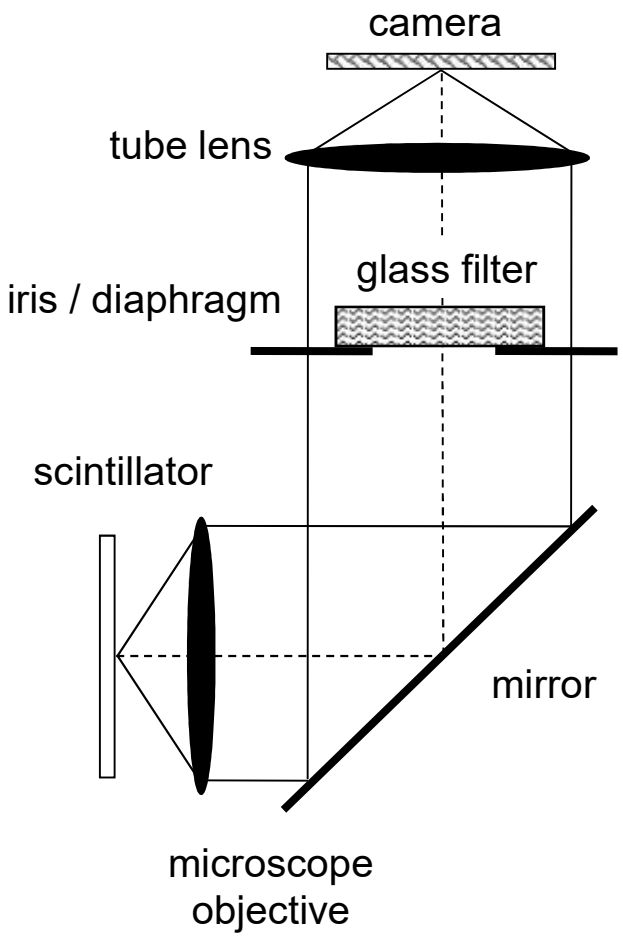

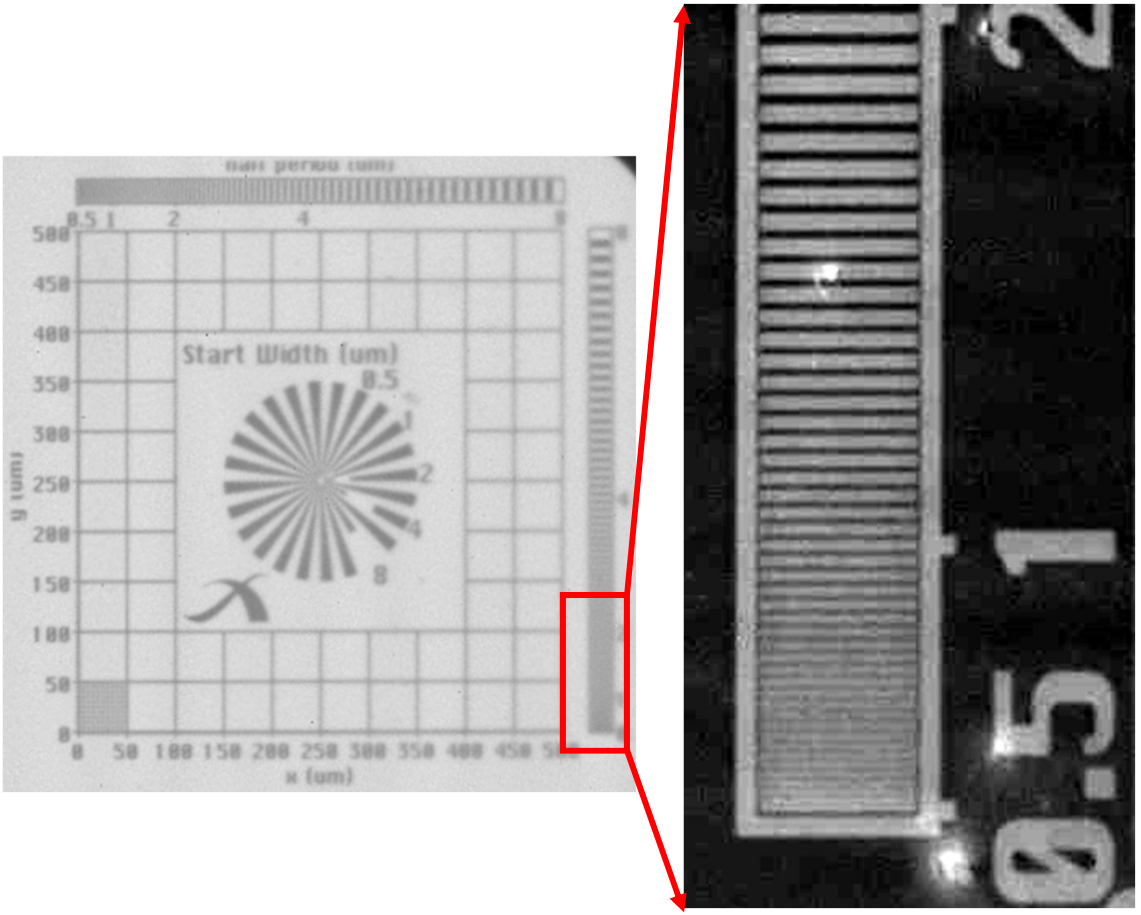

resolution, efficiency

Rack et al., Nucl Instr Meth B 267 (2009)

The Scientific Case of Metal Foams

METALLIC FOAMS

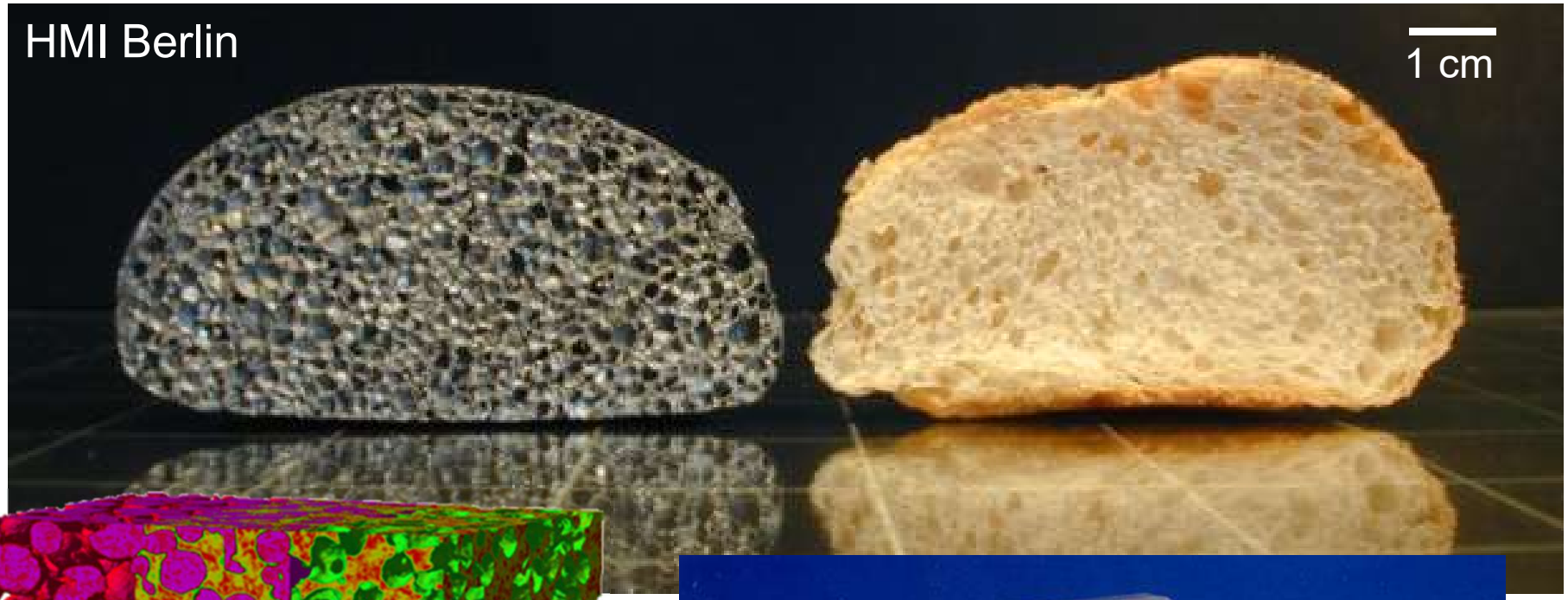

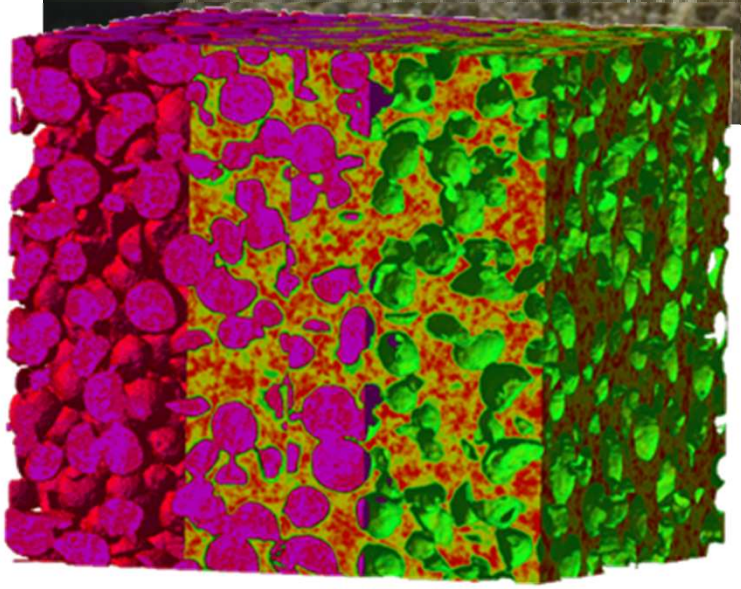

METALLIC FOAMS: POWDER-BASED PRODUCTION ROUTE

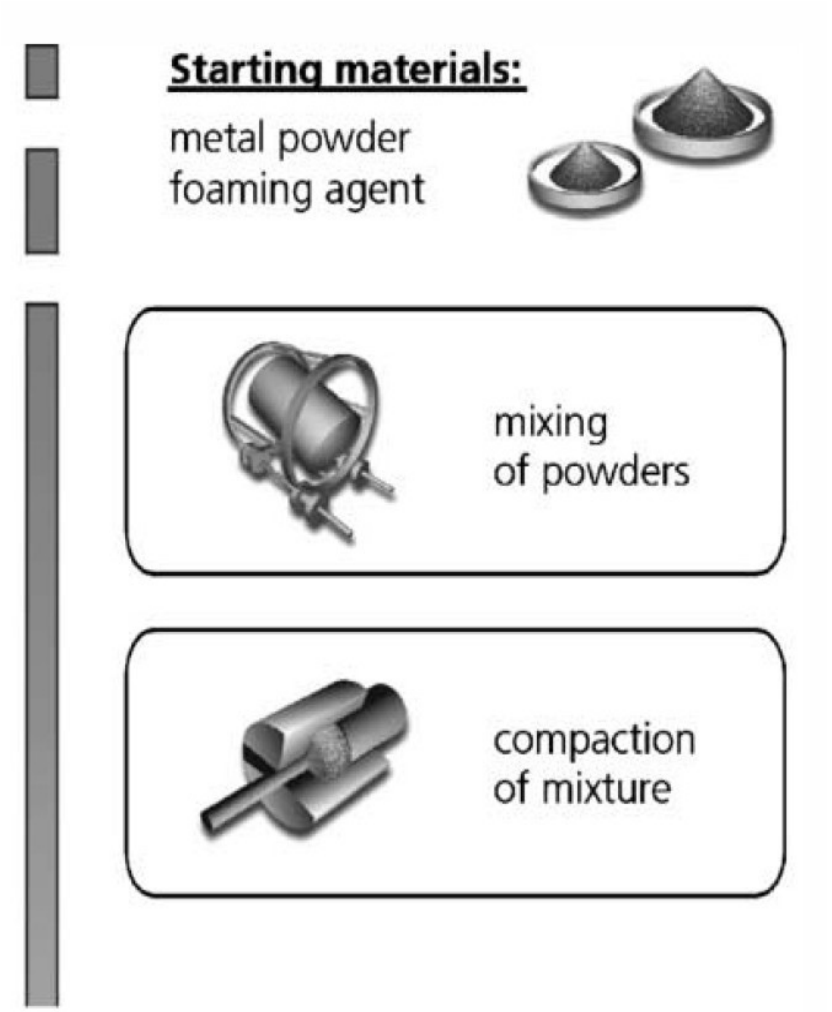

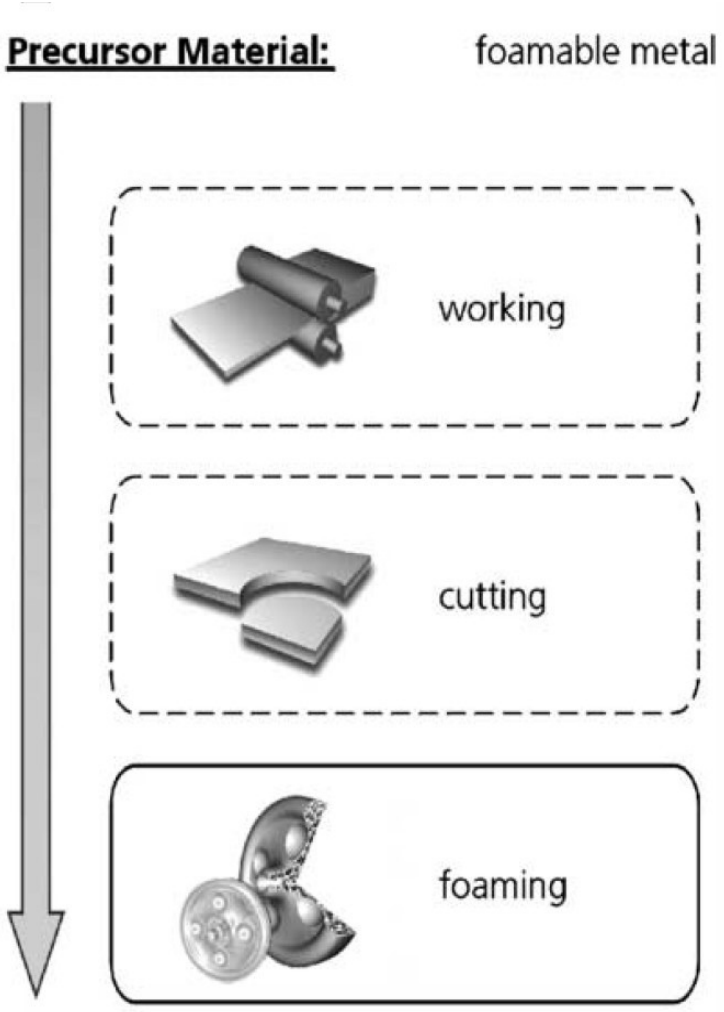

J. Banhart, Prog Mat Sci (2001)

METALLIC FOAMS: MICROTOMOGRAPHY

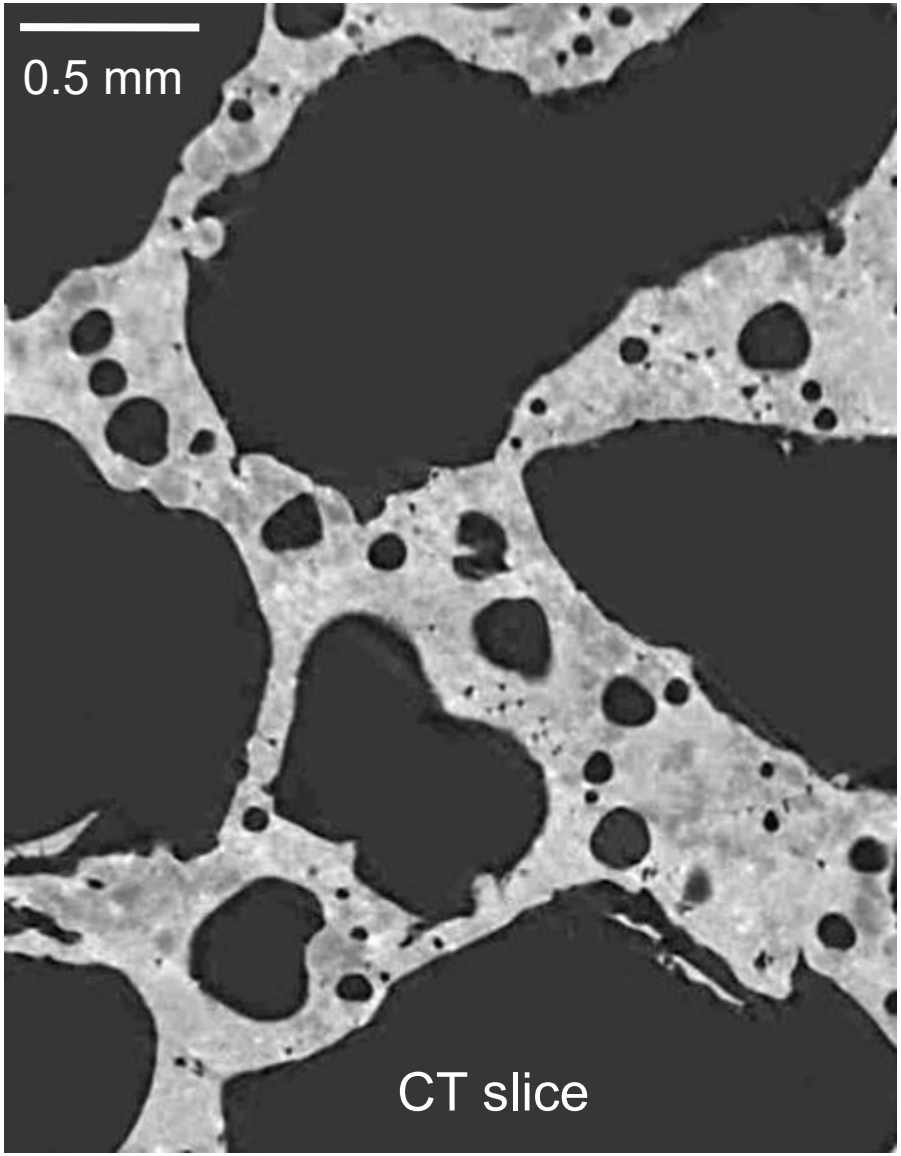

SEGMENTED VOLUME IMAGES

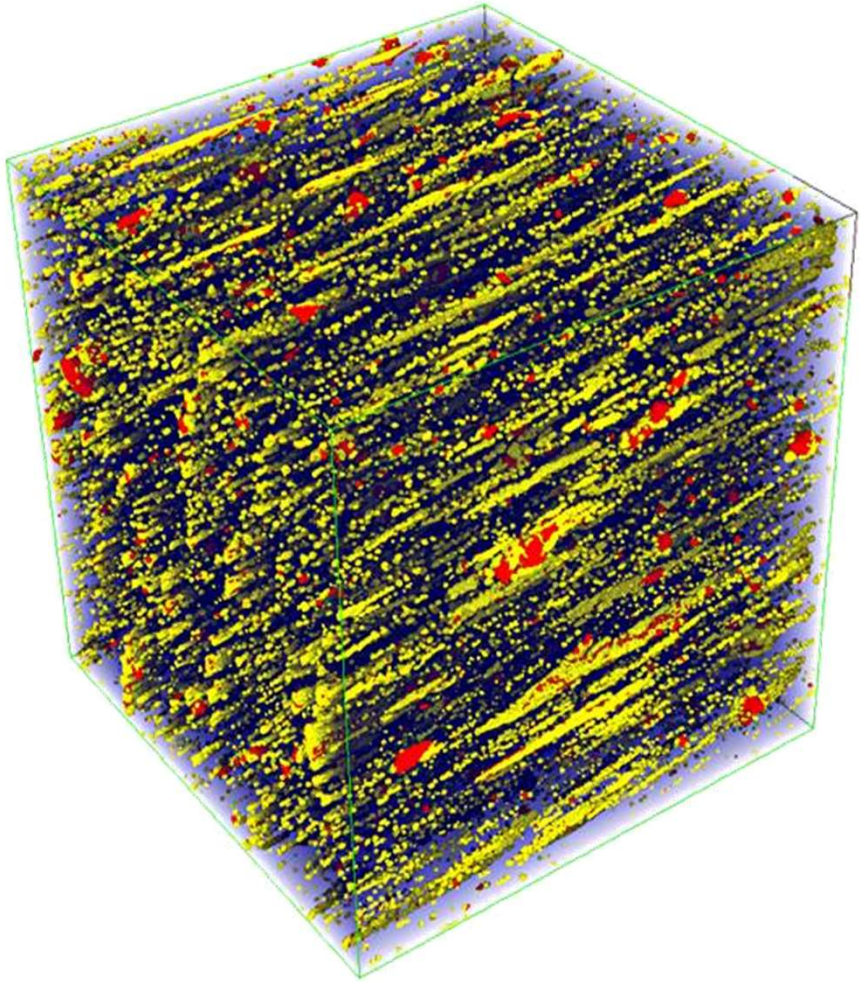

Al6061 (commercial AlSi alloy)

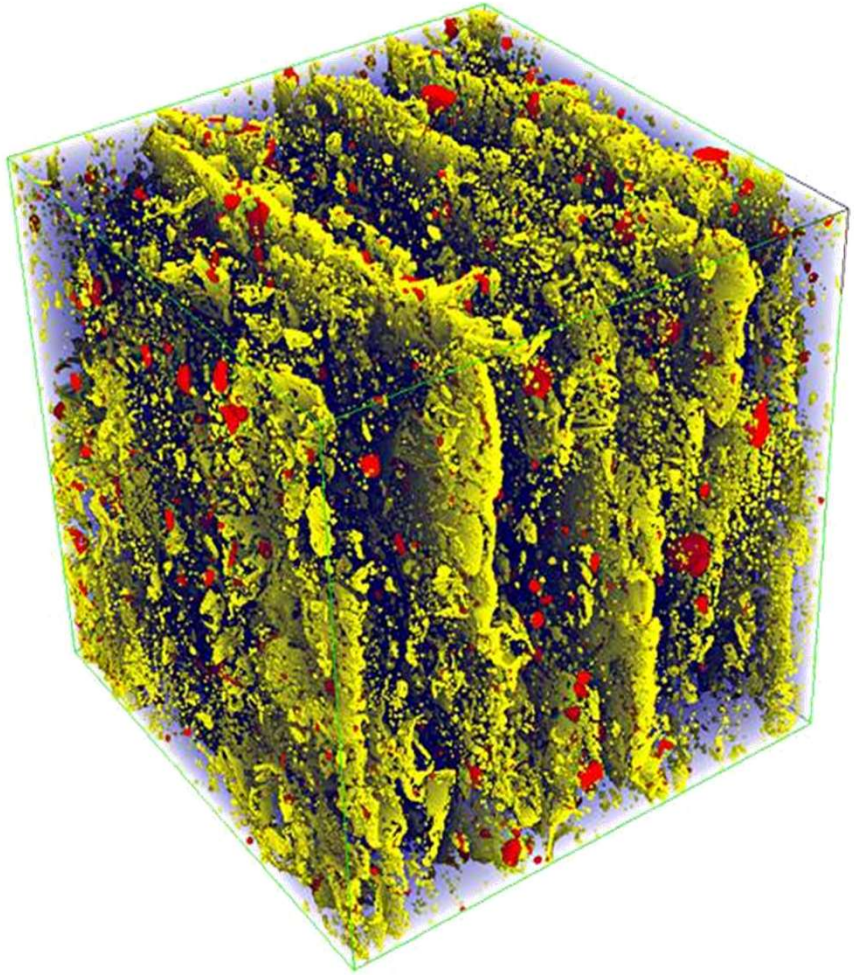

AlSi7 (elemental Al-Si mixture)

ANALYSIS: SPATIAL CORRELATIONS

pore dilation + calculation of the particle density found in each poor neighborhood

decreasing/increasing particle density

correlation/negative-correlation

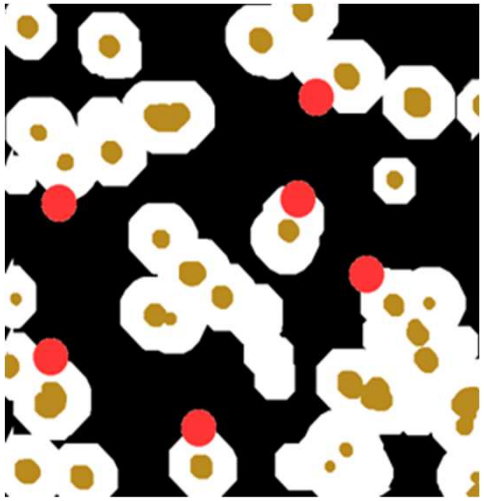

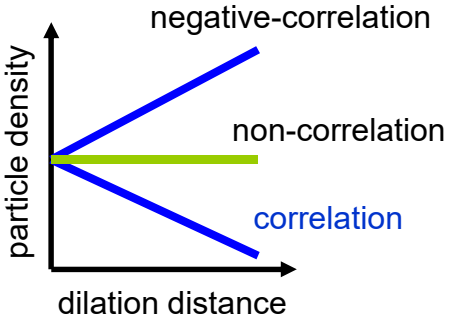

particle pores

pore neighborhood

Helfen, Ohser, Schladitz et al., Proc. SPIE 2003

constant particle density

non-correlation

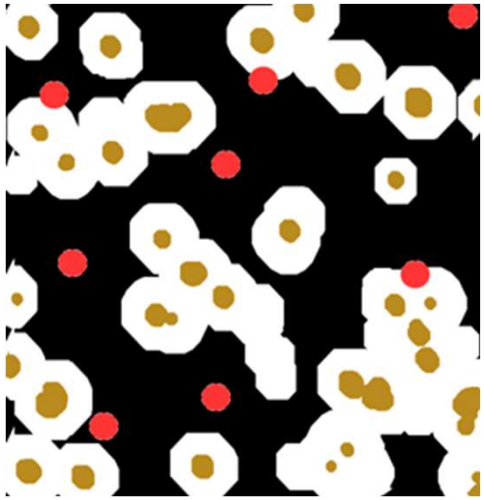

IMAGE ANALYSIS: PORE SPACE DILATION USING DISTANCE MAPS

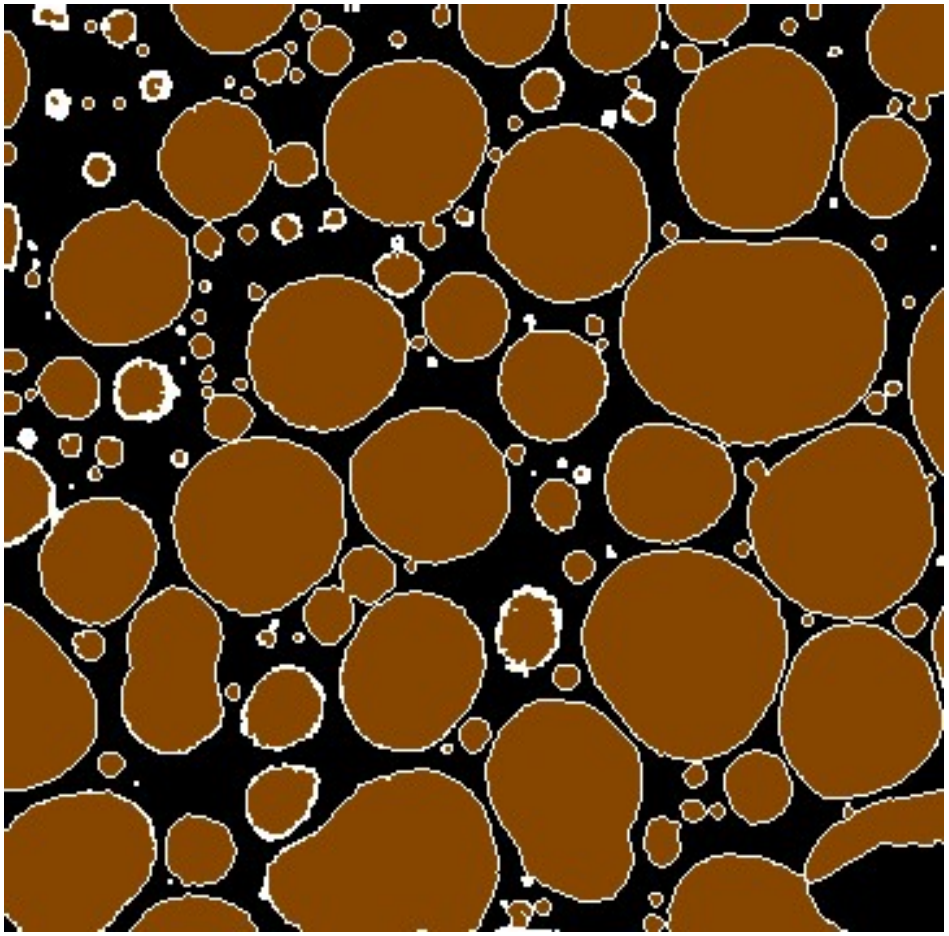

First dilation step

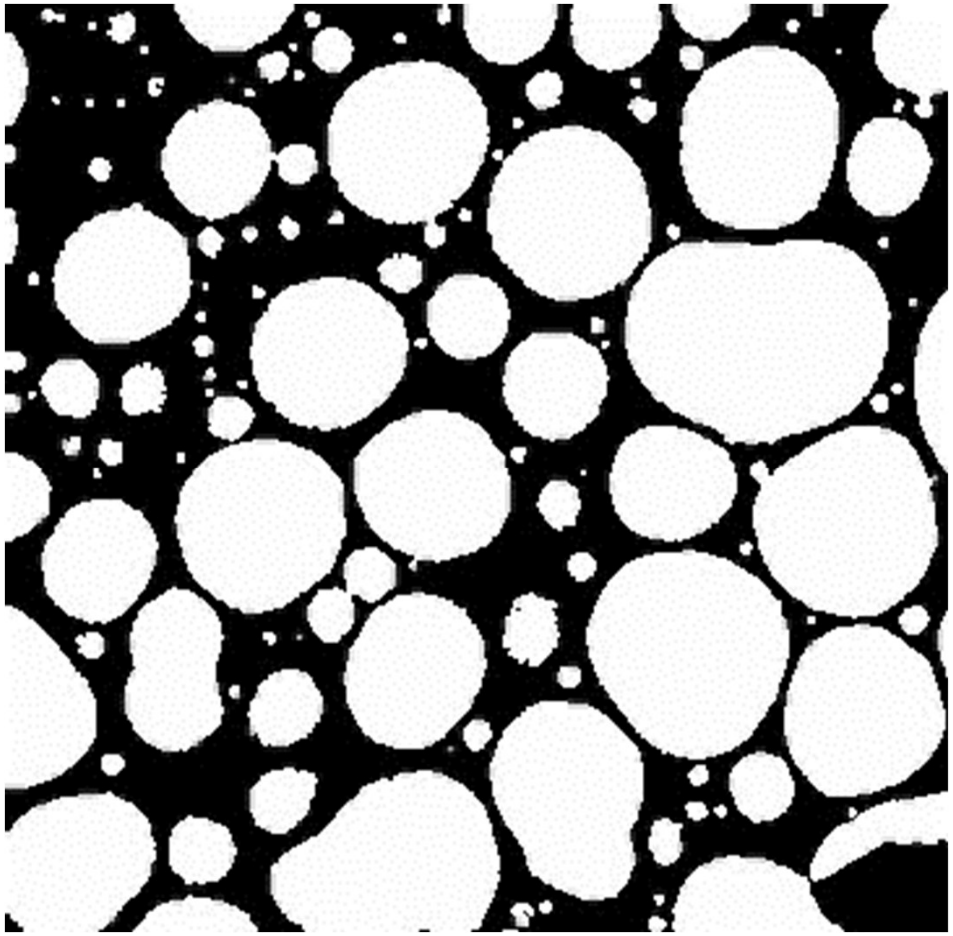

Dilation of pore volume in successive steps

SPATIAL CORRELATIONS: Al6061 vs. AlSi7

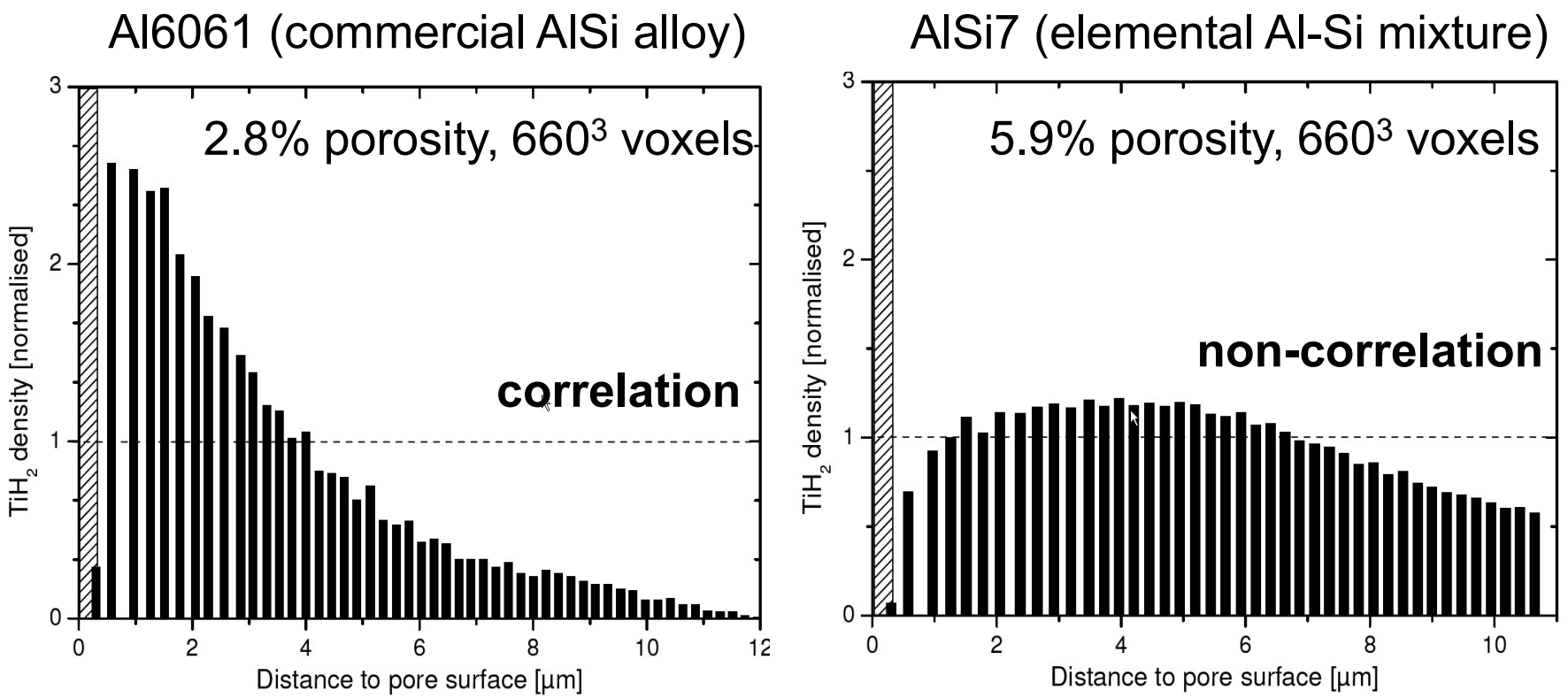

Rack, Ohser, Schladitz, Helfen et al., Journal Microscopy 232, 2008

METALLOGRAPHIC IMAGE AlSi7

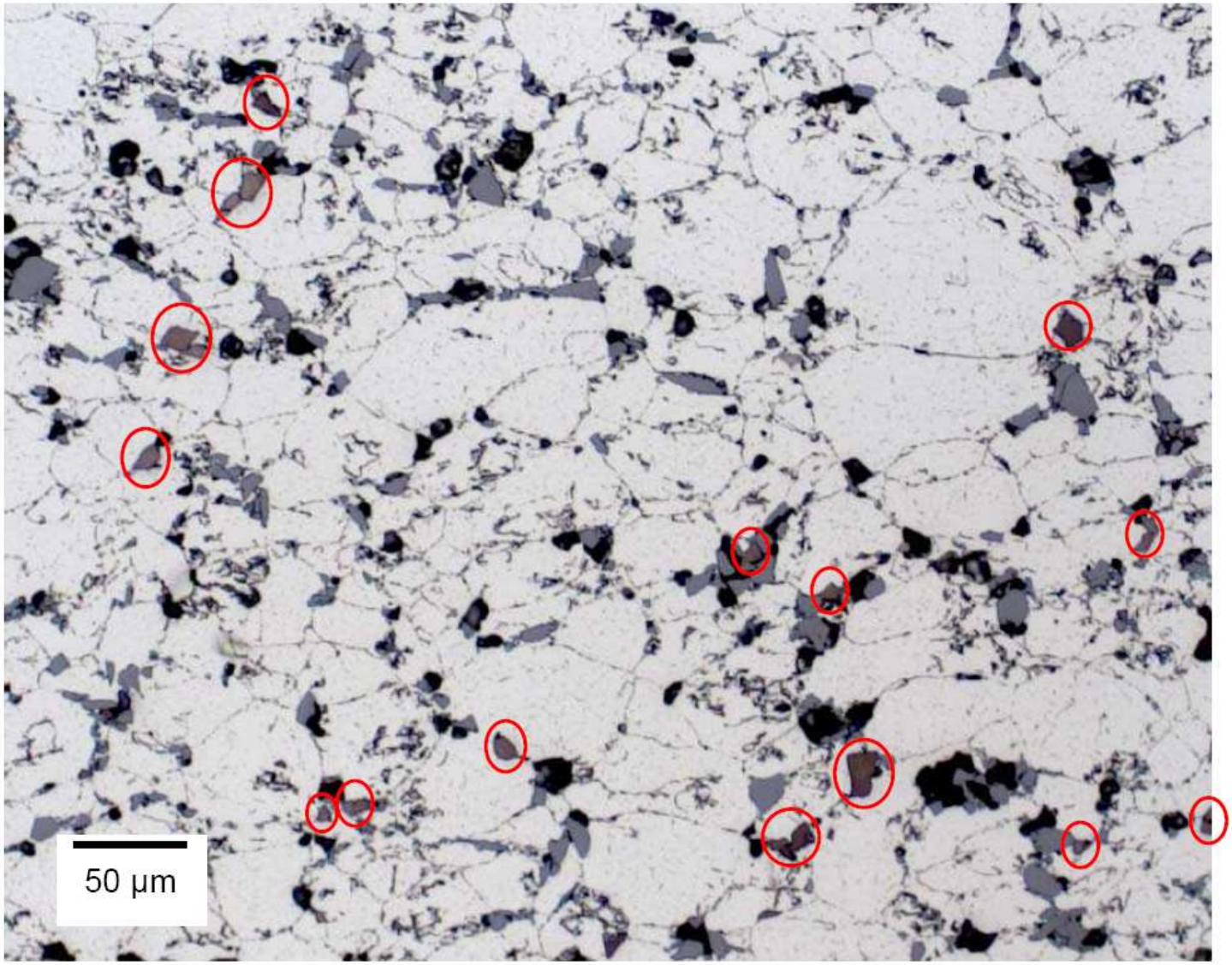

Rack et al., Acta Materialia 52 (2009)

METALLIC FOAMS: AlSiCu

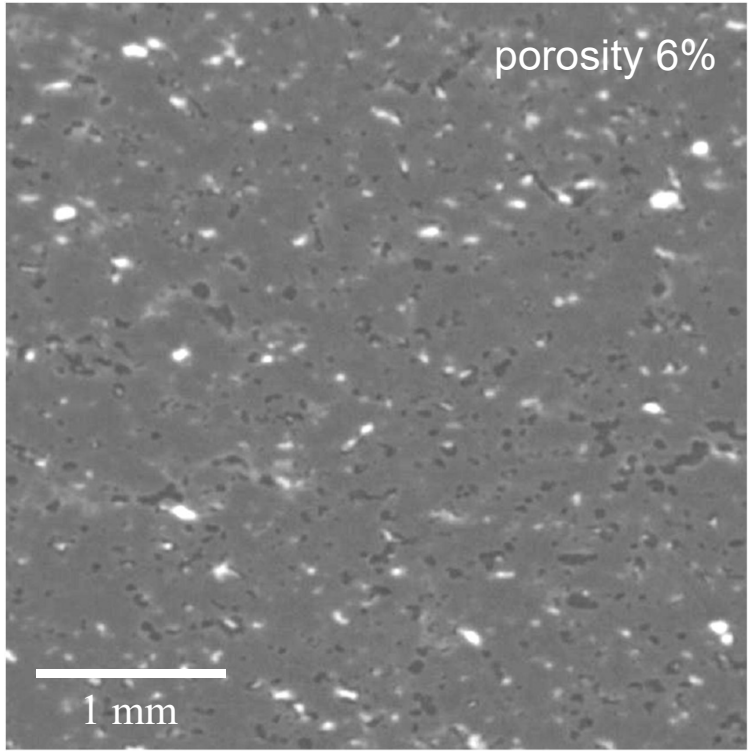

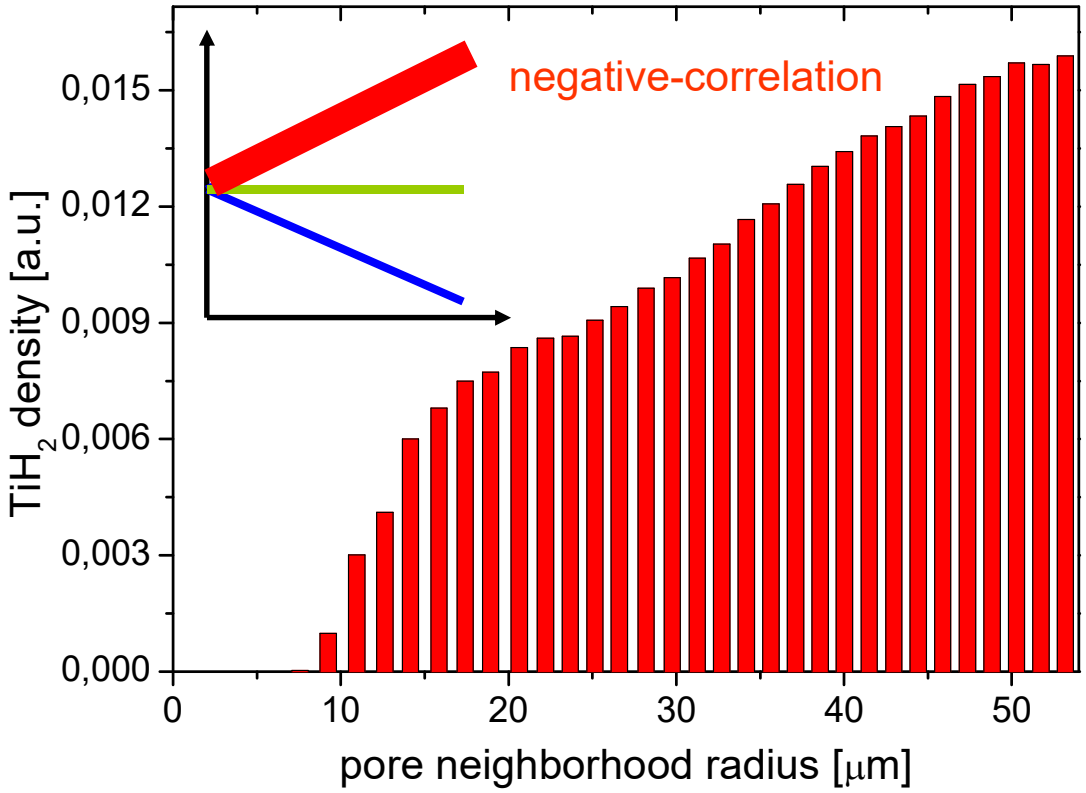

Rack et al., Acta Materialia 52 (2009)

METALLIC FOAMS: AlSiCu

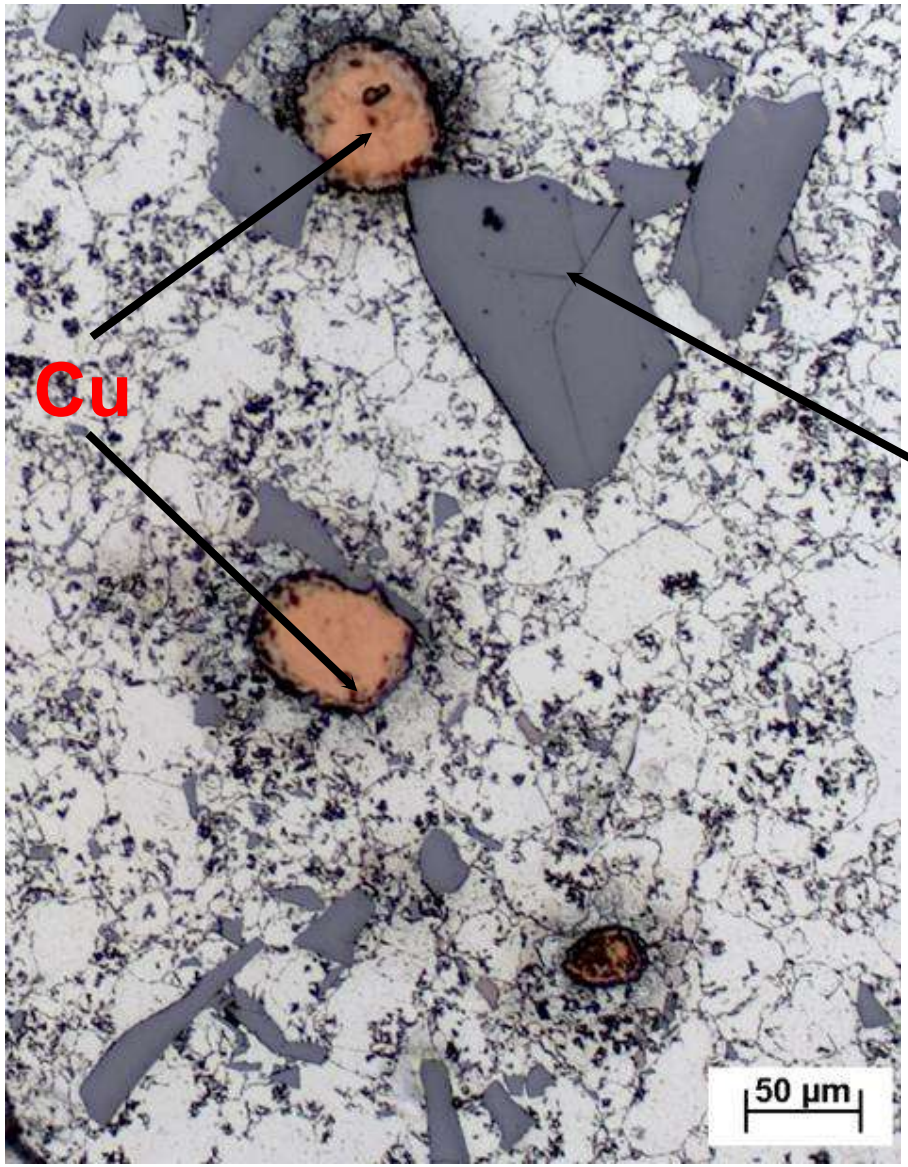

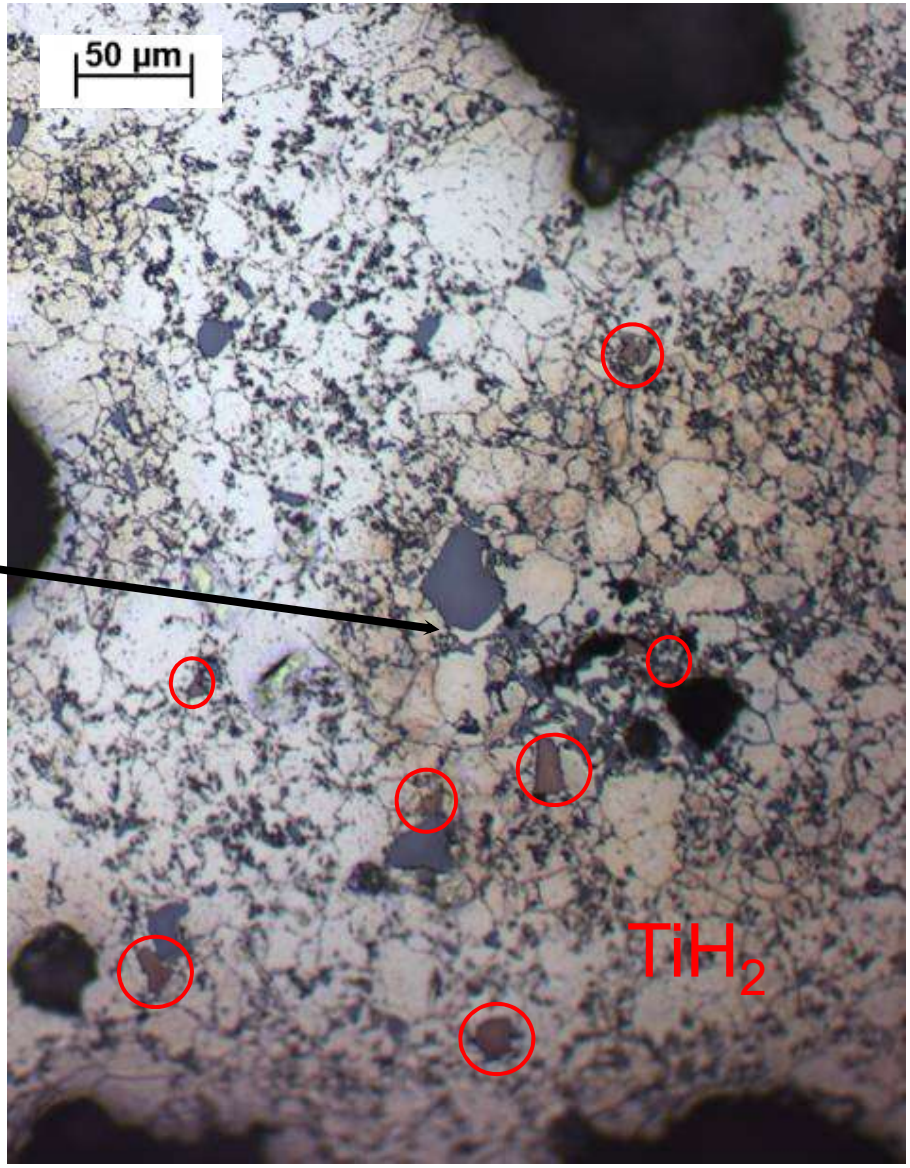

Exploiting Contrast with Tomography
- Synchrotron Light Sources, Scanning Techniques -

SYNCHROTRON LIGHT SOURCES

SYNCHROTRON LIGHT

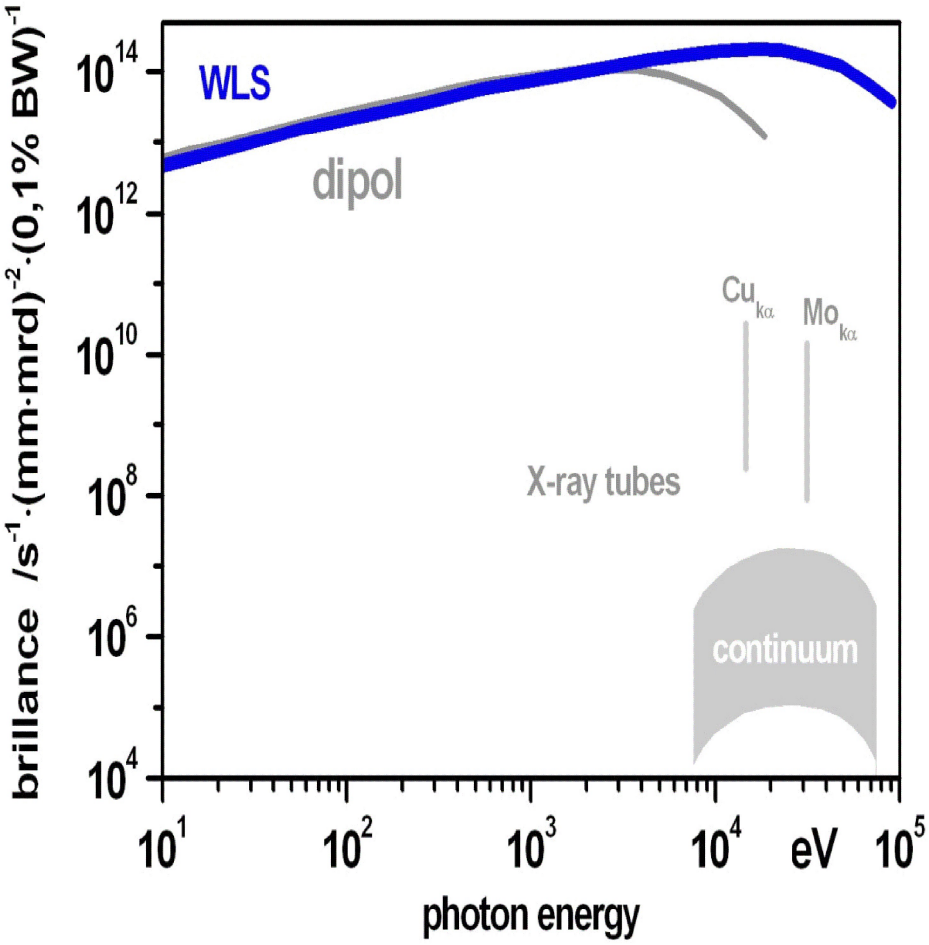

B.R. Müller et al., DGZfP 2005

- higher flux → allows the use monochromators:
  - higher contrast
  - no beamhardening artifacts
- quasi parallel beam
- partial spatial coherence - use of different contrast modes for higher sensitivity, e.g. the local electron density (holo-CT)

<u>but:</u>

- relative expensive
- only limited amount of beamtime available

PERIPLANETA AMERICANA - FRONTAL

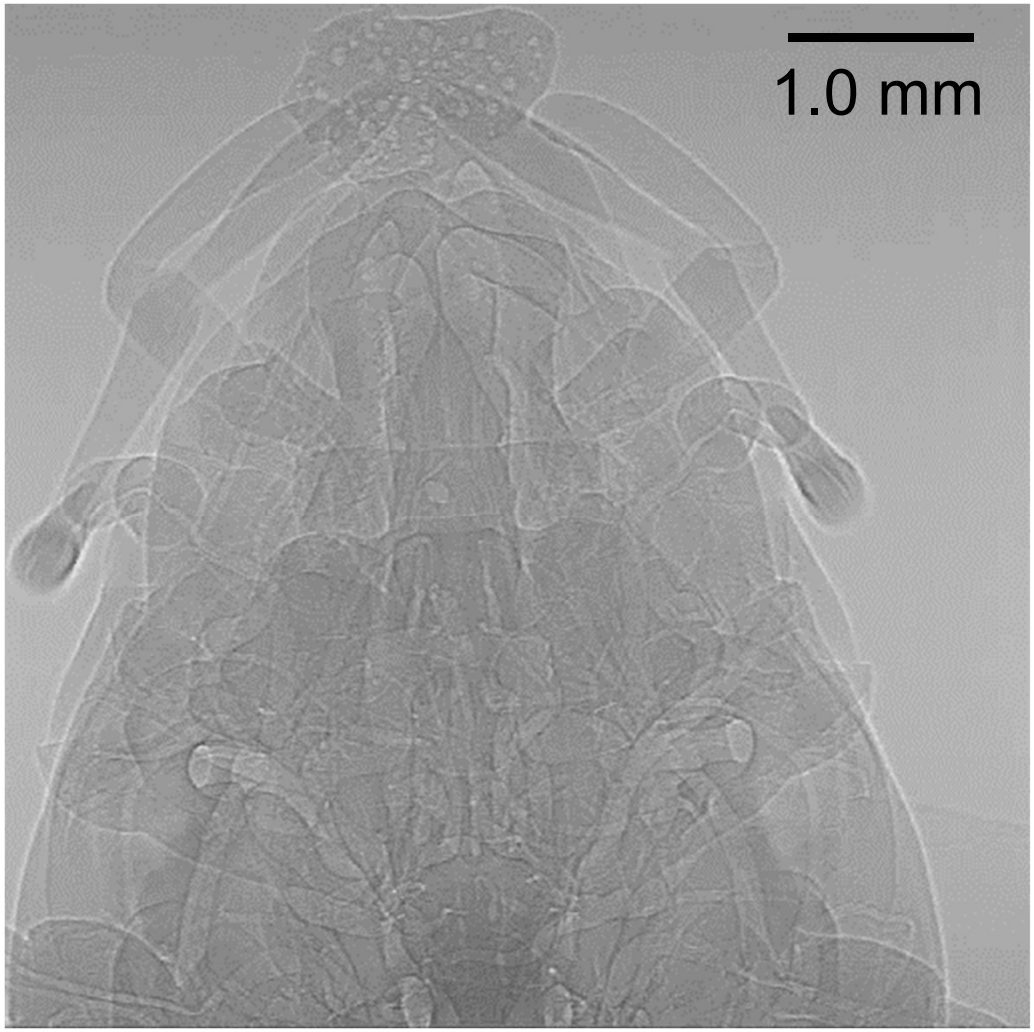

- mouthpart kinematics during feeding
- 125 FPS
- 15 µm spatial detector resolution
- Betz, Rack et al., Synch Rad News `08 & J. Exp. Biol. `14
- Westneat, Betz et al., Science `03
- TopoTomo @ ANKA

commercial Aluminum alloy A357 (Al, Si, Mg)

(18 keV, 0.8 µm pixel size / <2 µm resolution)

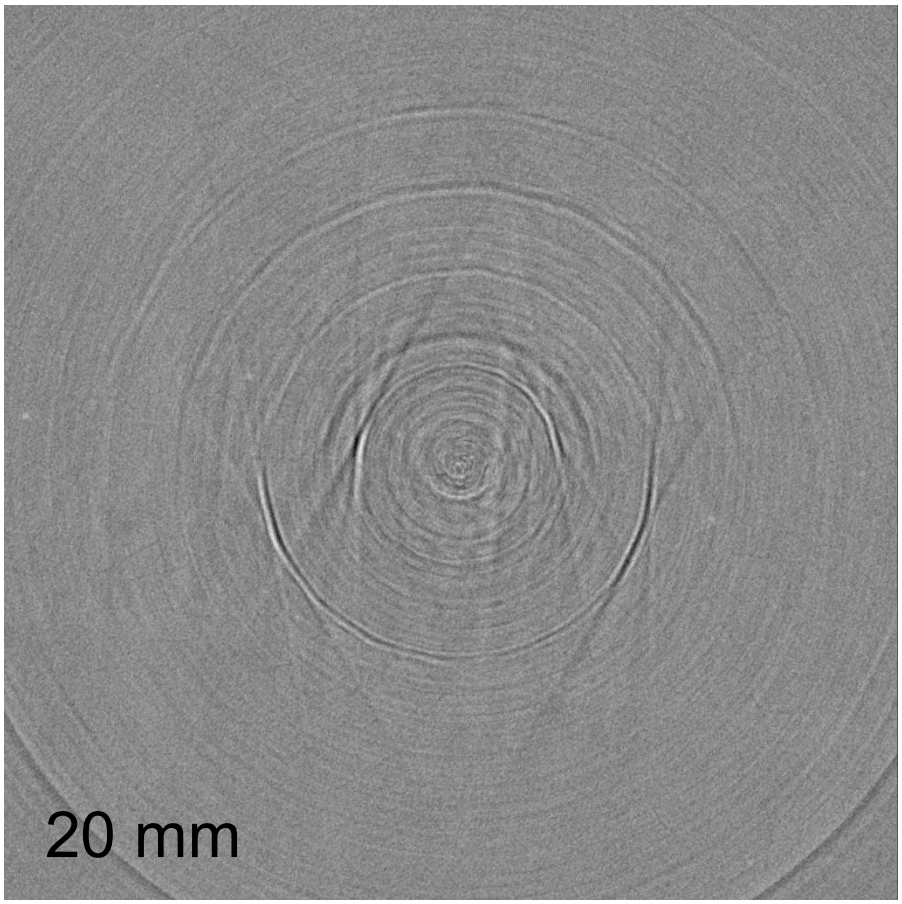

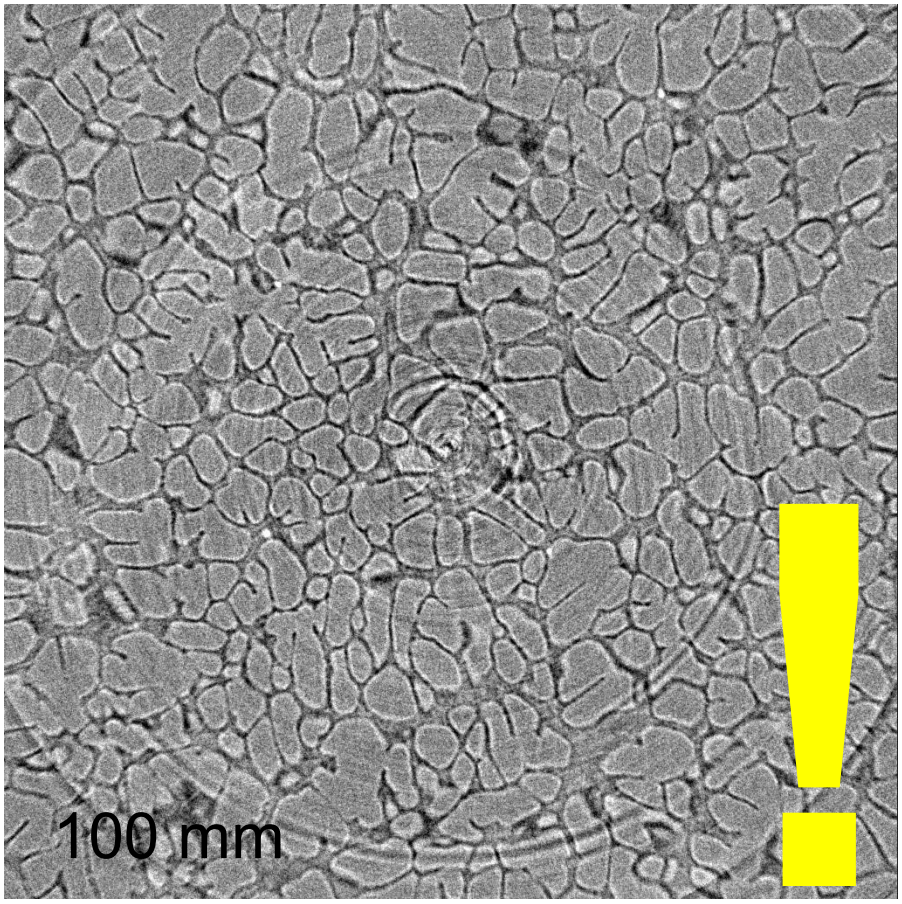

Simon Zabler, PhD thesis

HIGH ENERGY & HIGH RESOLUTION

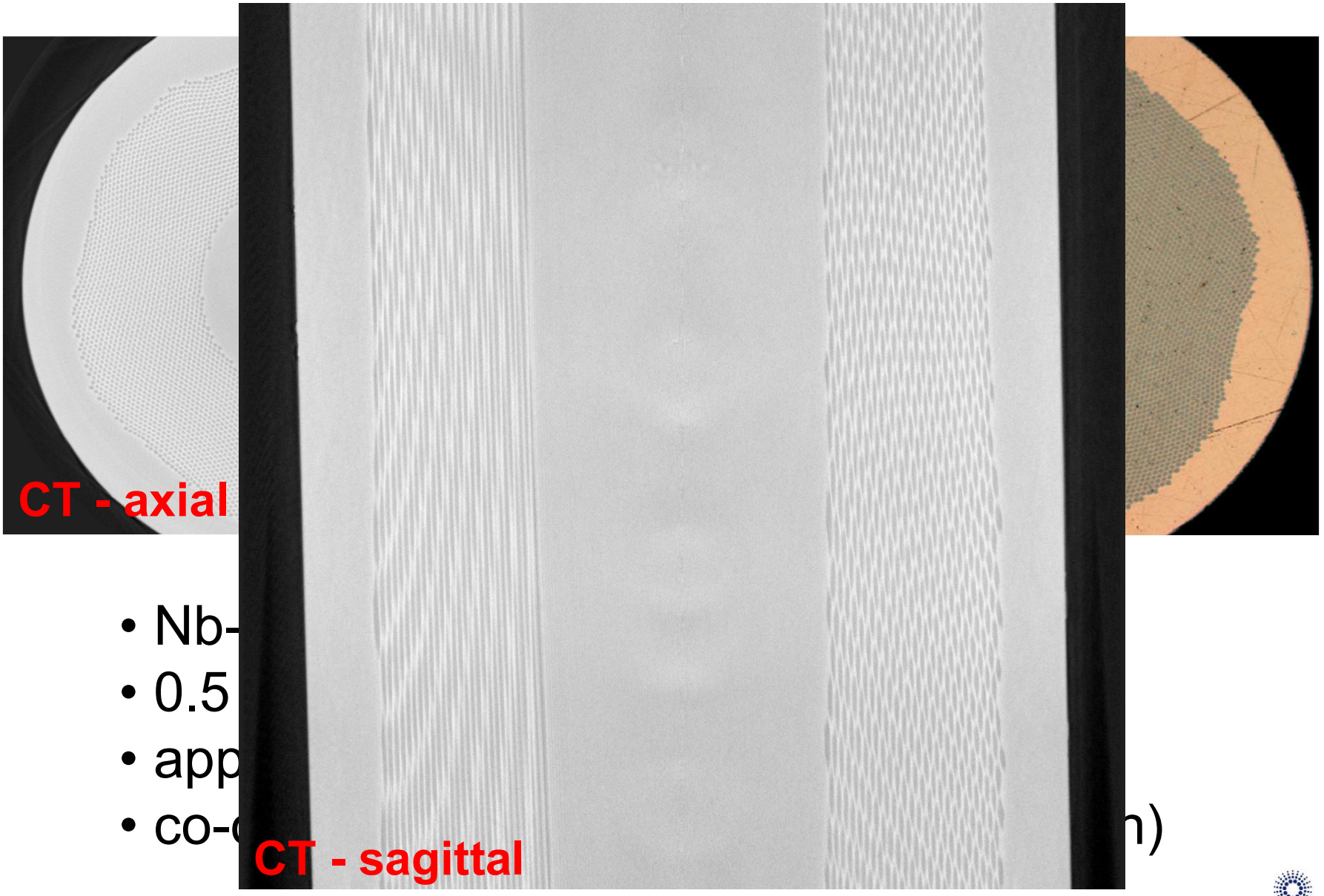

- Nb-
- 0.5
- app
- co-

n)

Diffraction Contrast Tomography

Conventional tomography setup, large detector with high dynamic range, use slits to confine the beam to sample, monochomatic beam ($\Delta\lambda/\lambda \sim 10^{-4}$), continuous rotation, large number of images (7200 /360°).

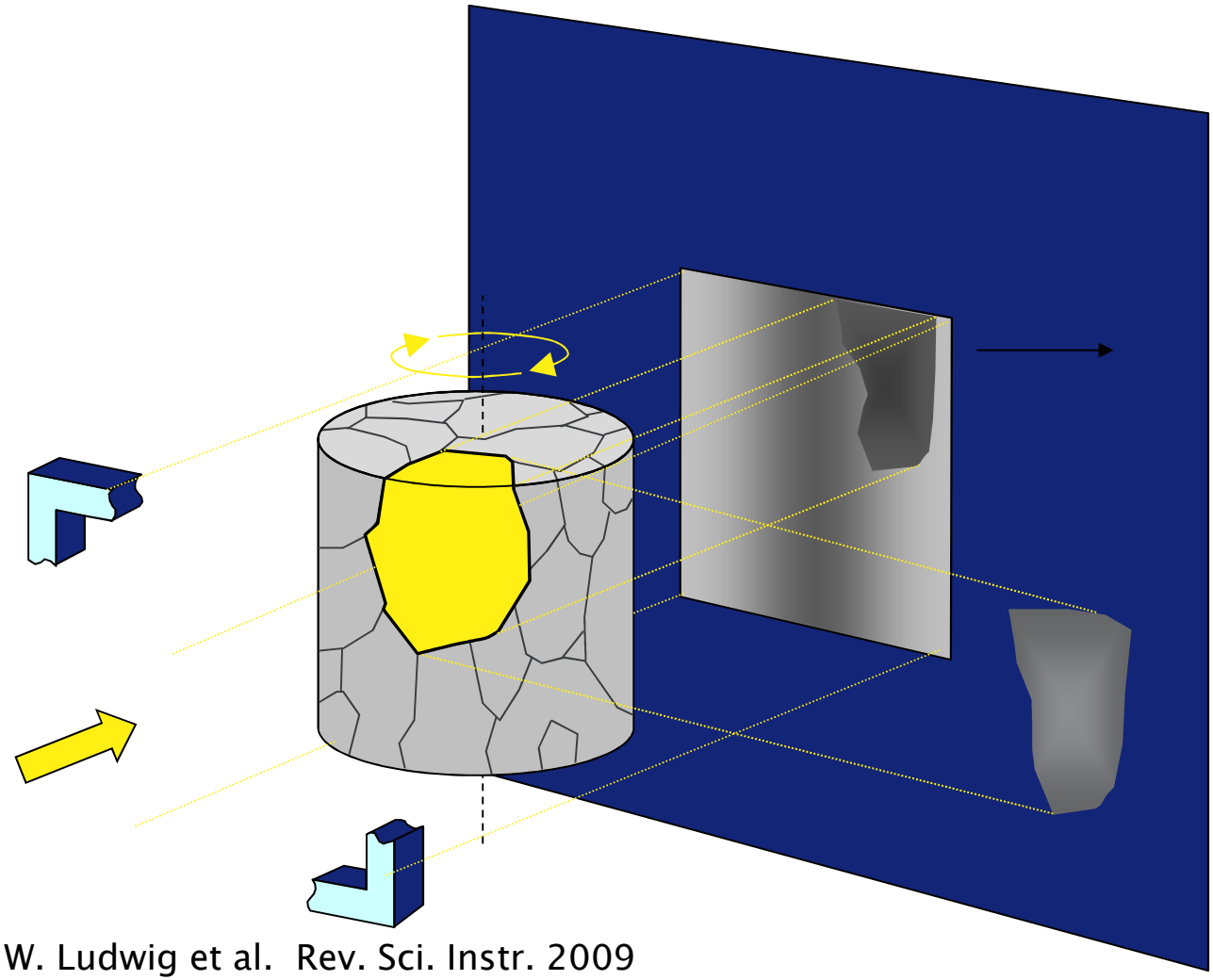

W. Ludwig et al. Rev. Sci. Instr. 2009

During rotation, grains pass through Diffracting alignments

grains with small spreads in orientation:

"extinction" spot visible in direct beam

both spots can be approximated as grain projections

Diffraction Contrast Tomography

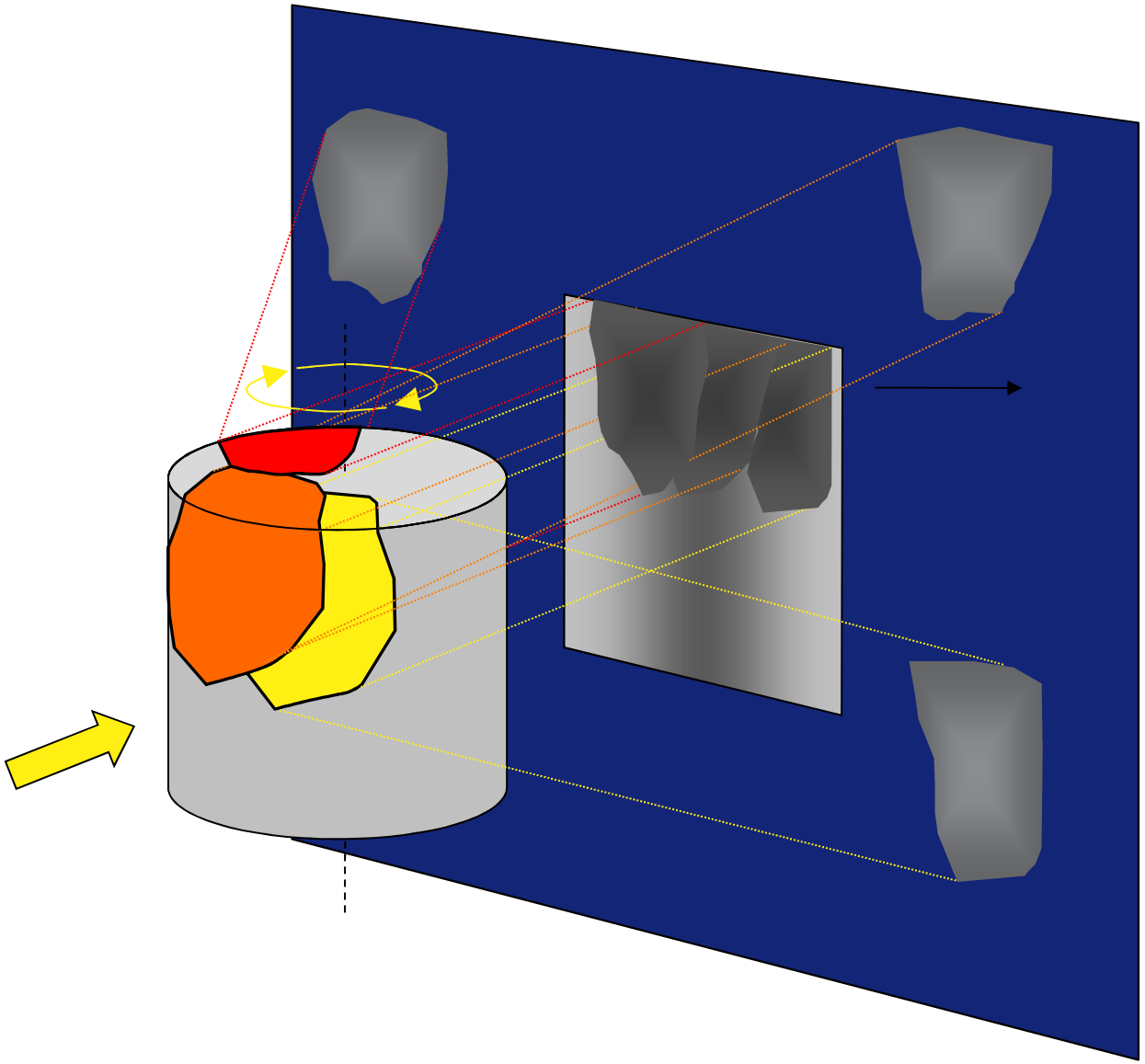

During sample rotation should see each grain ~ 20 - 100 times.

Some may be lost

Overlaps

Off the detector

Low contrast

Enough to reveal the 3D grain shape through ART reconstruction

DCT - Indexing

uses spatial (common center of mass, shape, etc..) and crystallographic constraints (interplanar angles)

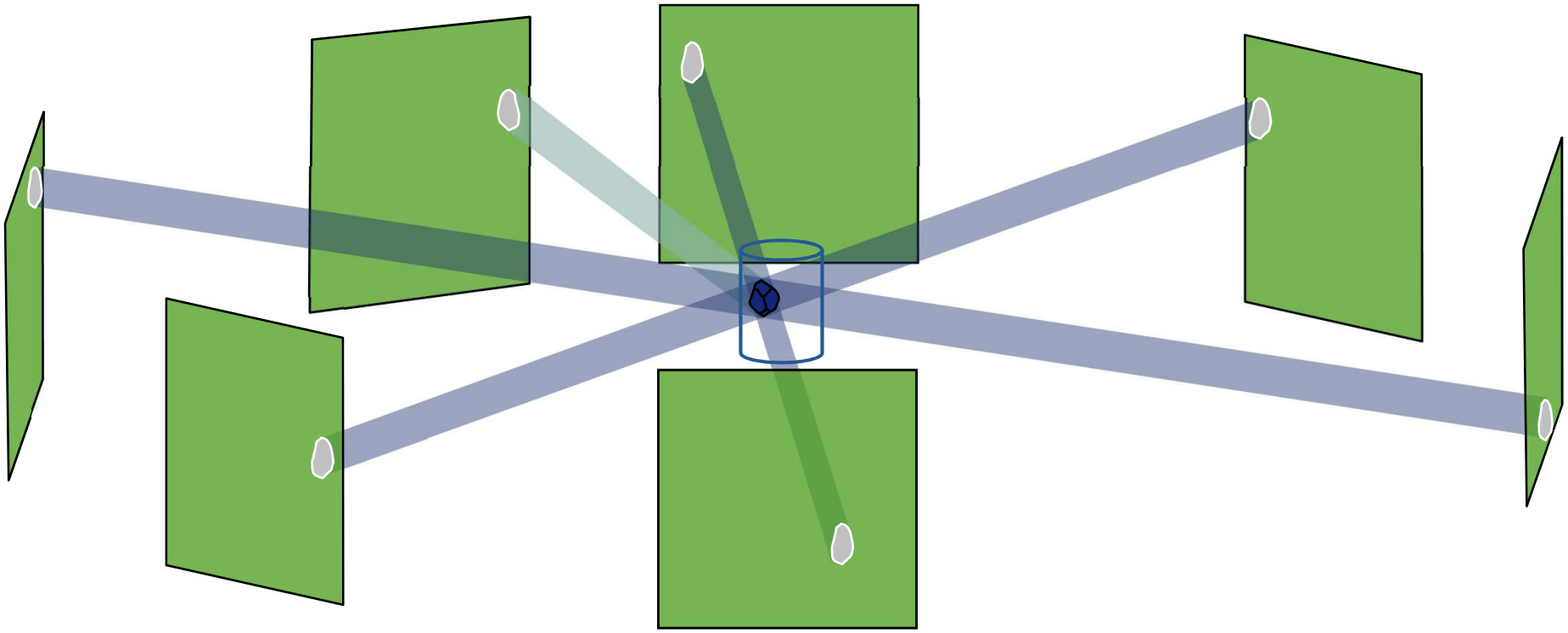

Chironex fleckeri

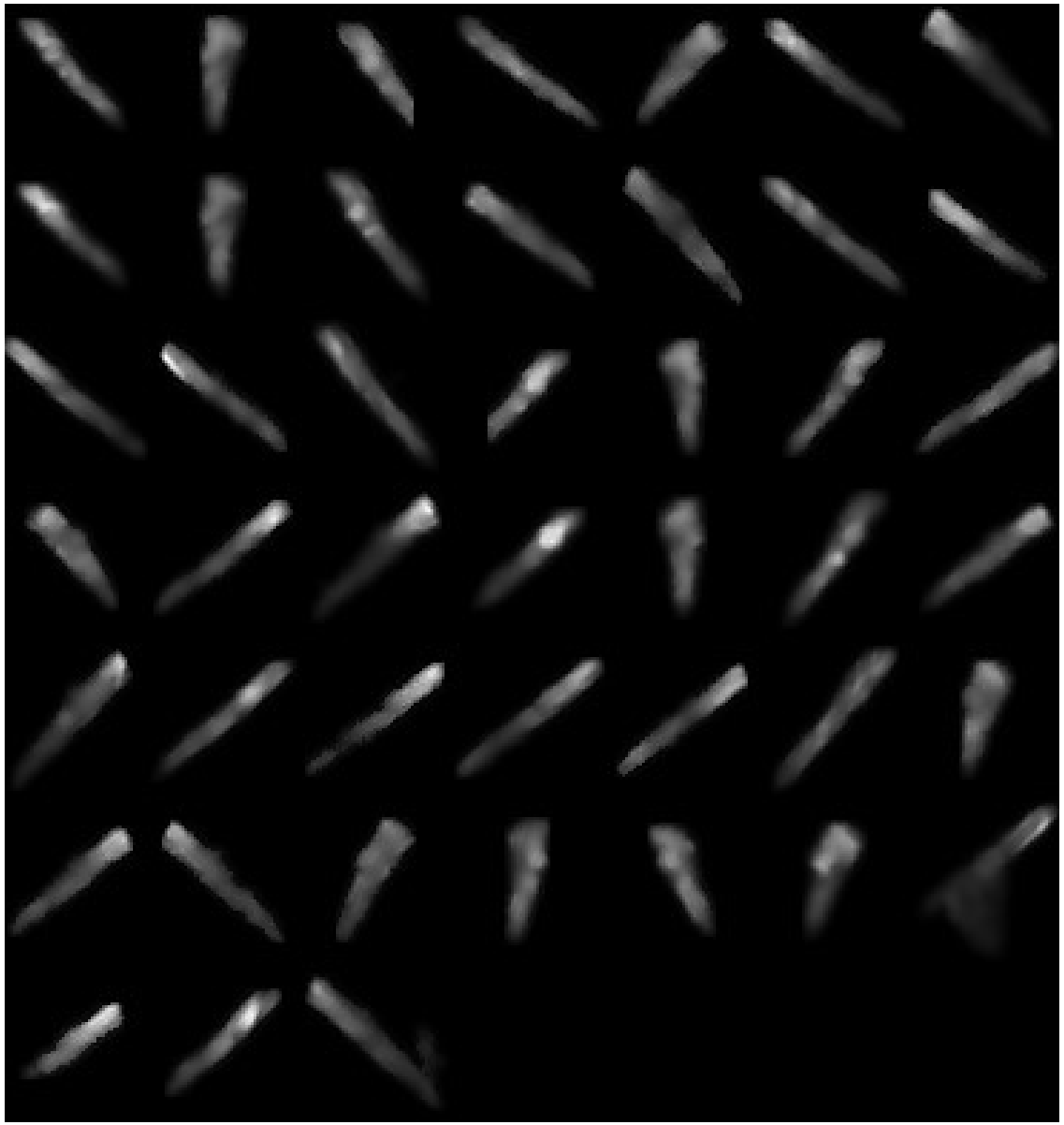

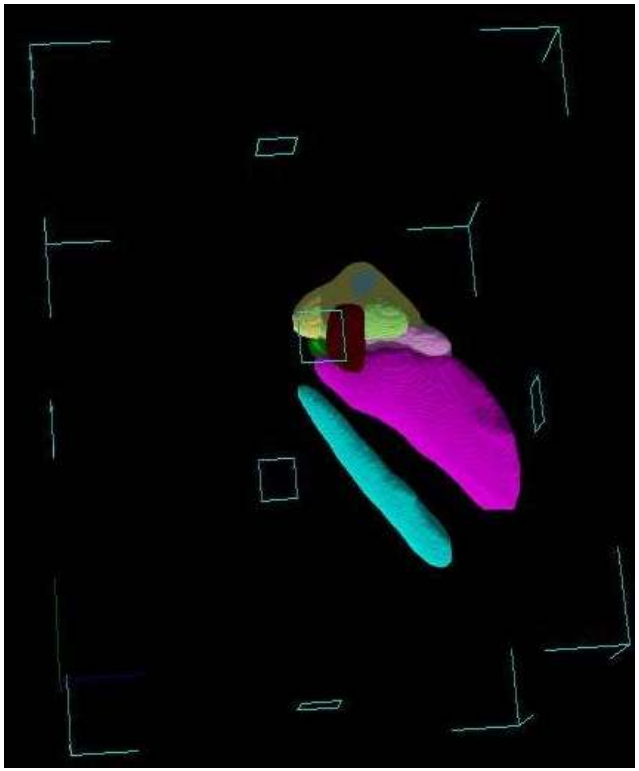

Sötje et al., Marine Biology (2009)

Multi-modal contrast: scanning techniques with tomography

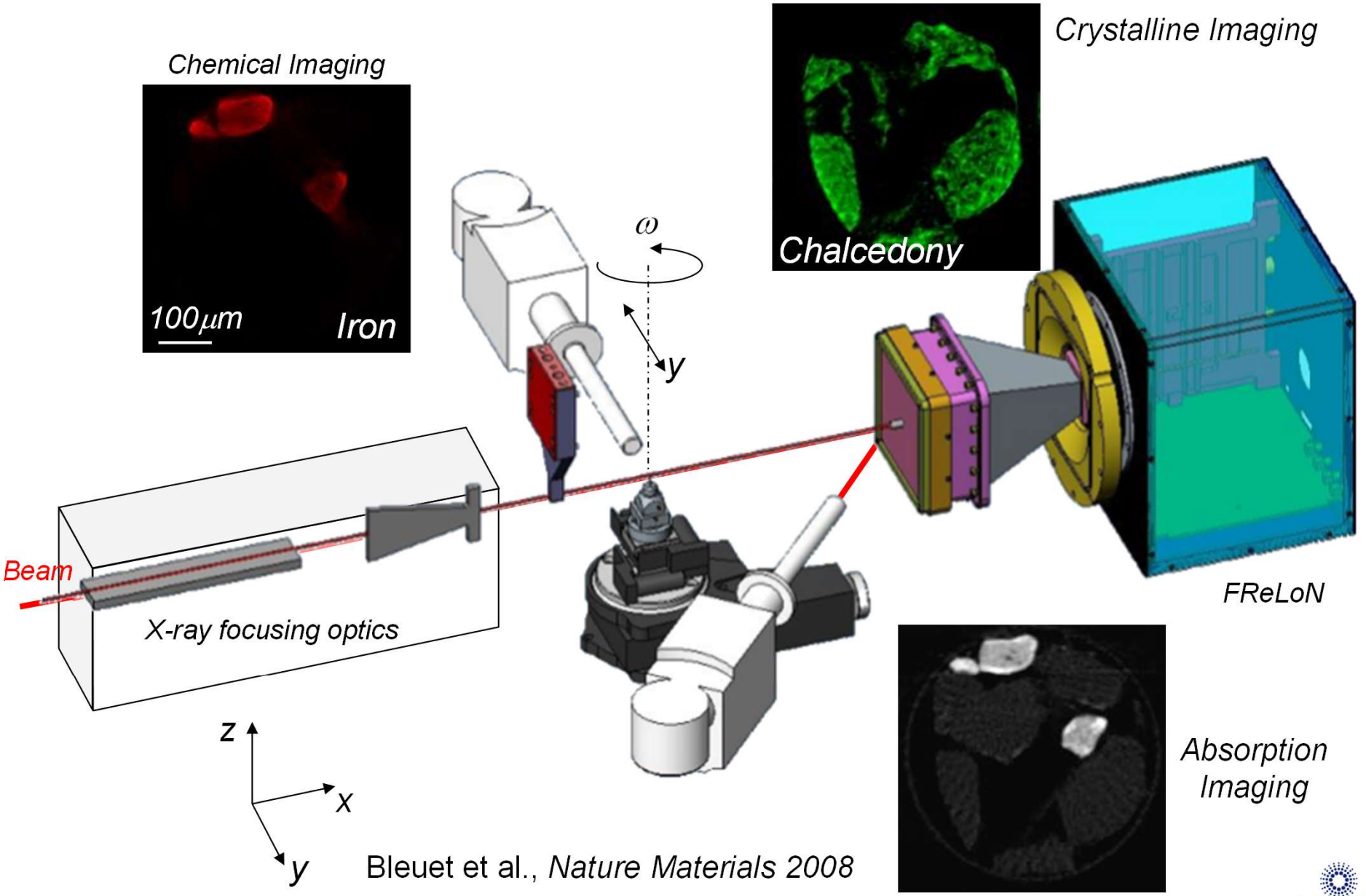

Bleuet et al., *Nature Materials 2008*

X-RAY FLUORESCENCE TOMOGRAPHY

$$\int \alpha . p_{fluorescence(Z)}(s,u)du$$

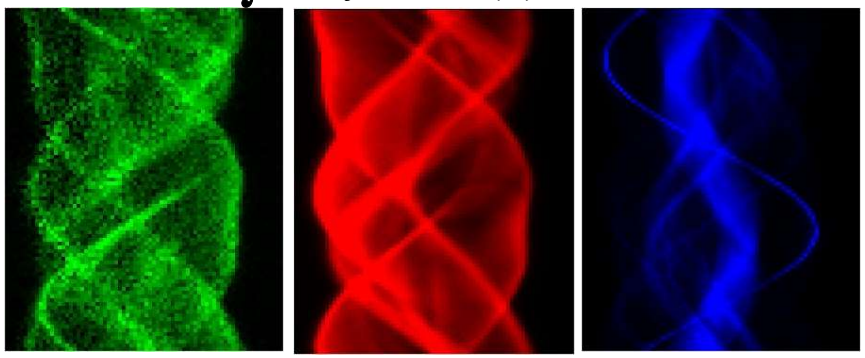

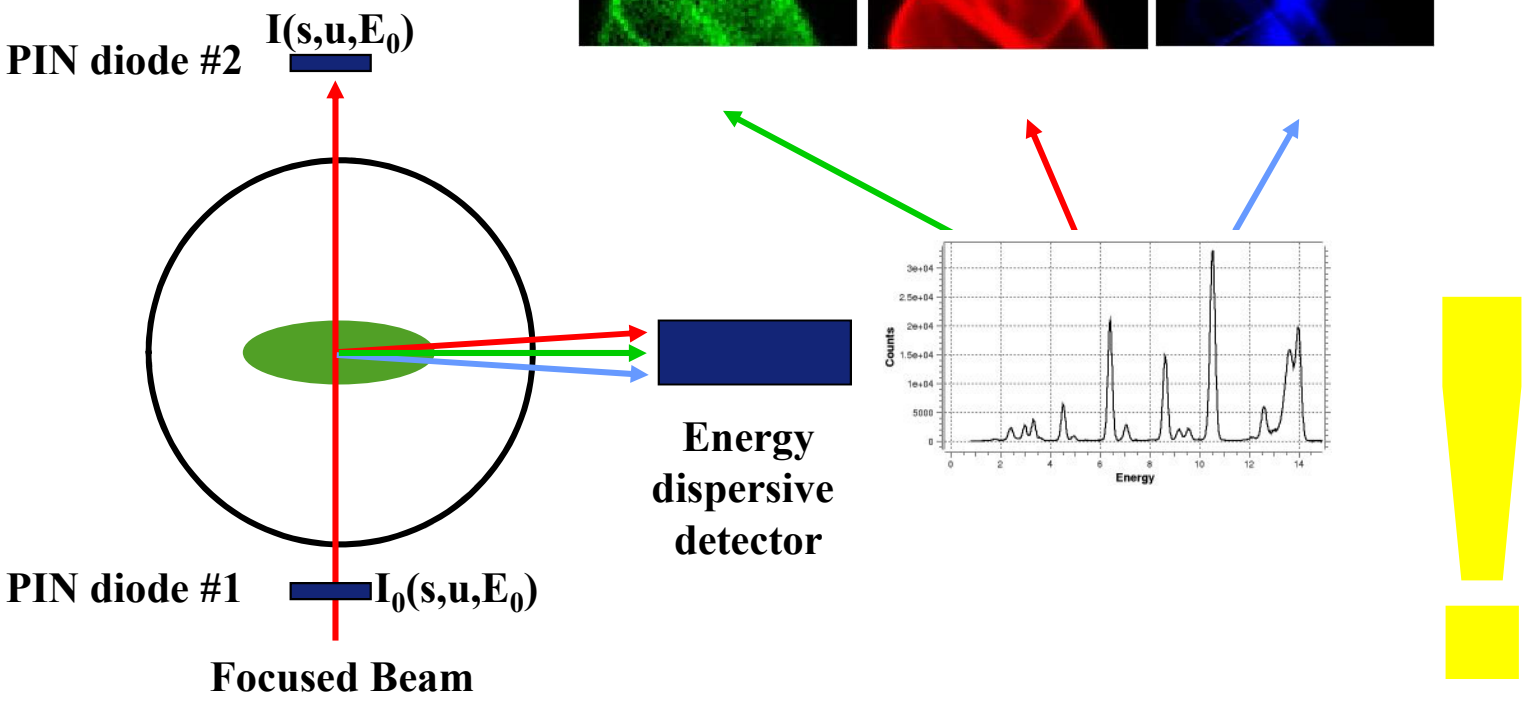

Bleuet et al., *SPIE*, 2006

X-RAY FLUORESCENCE TOMOGRAPHY

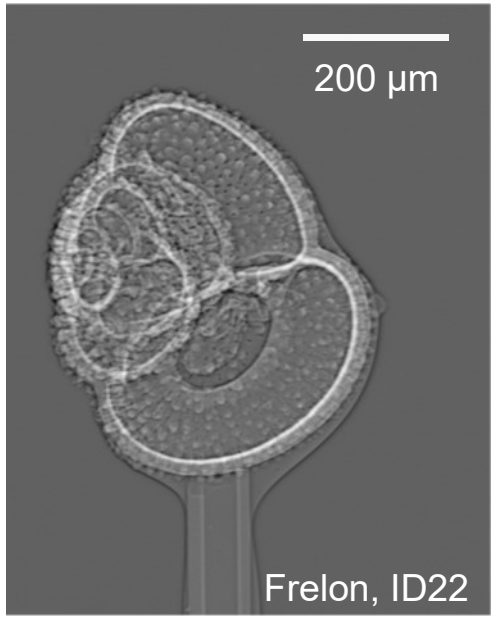

S

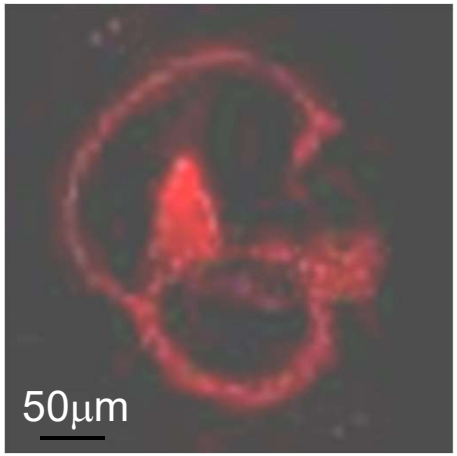

Cl

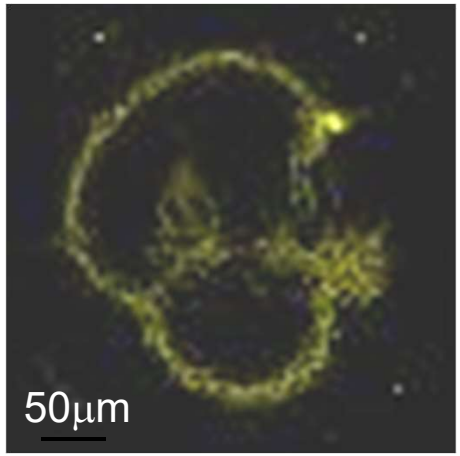

Ca

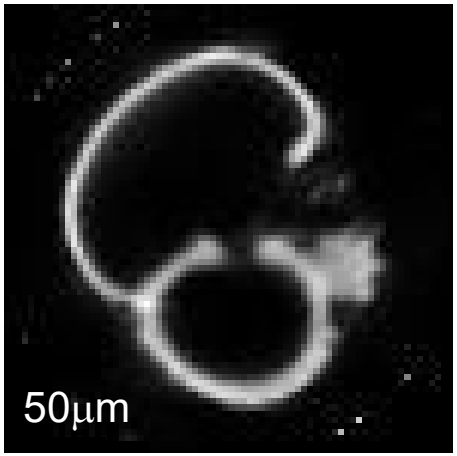

Cu

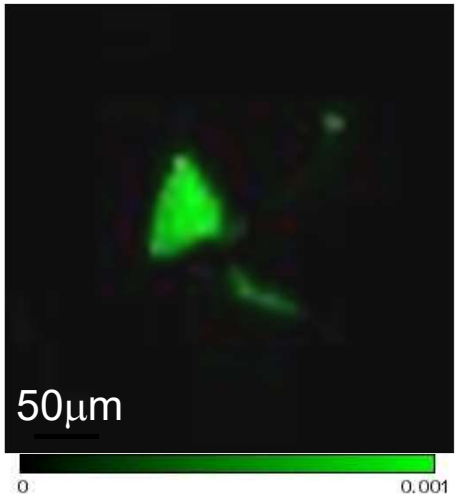

Zn

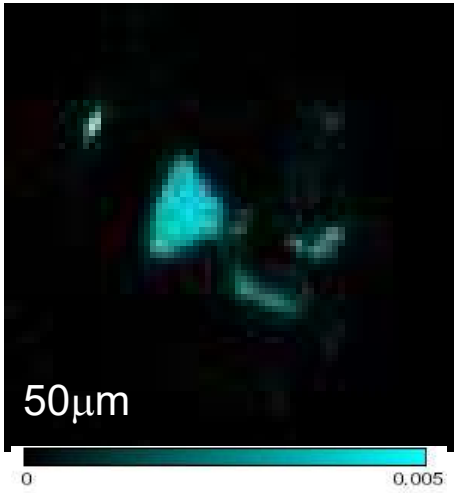

Access to the internal chemical distribution

Bleuet et al., *SPIE*, 2006

Scanning CT: Reconstruction Scheme

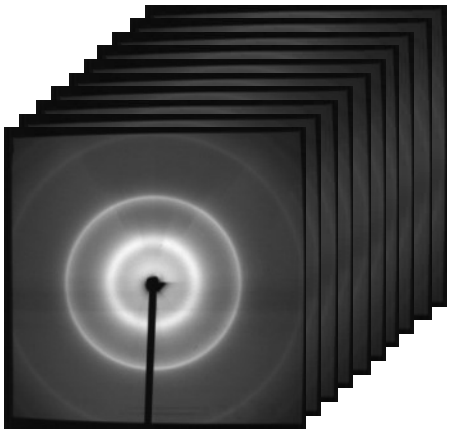

$N_y \times N_\omega$ Diffraction Images

Azimuthal Integrations

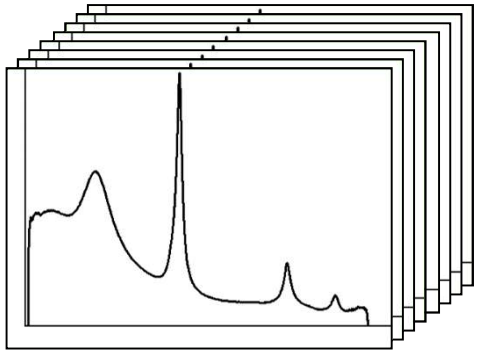

$N_y \times N_\omega$ Diffraction Patterns

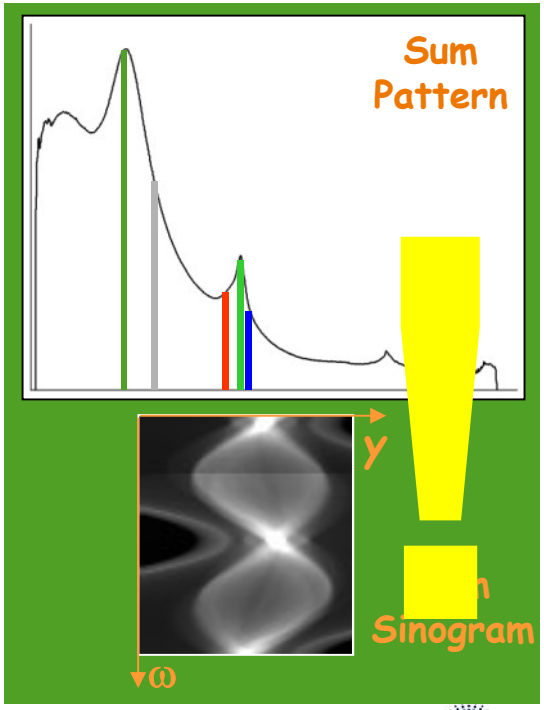

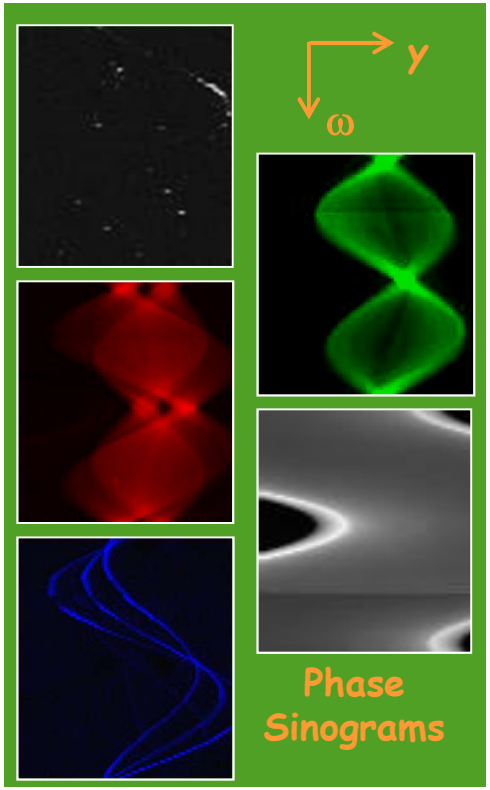

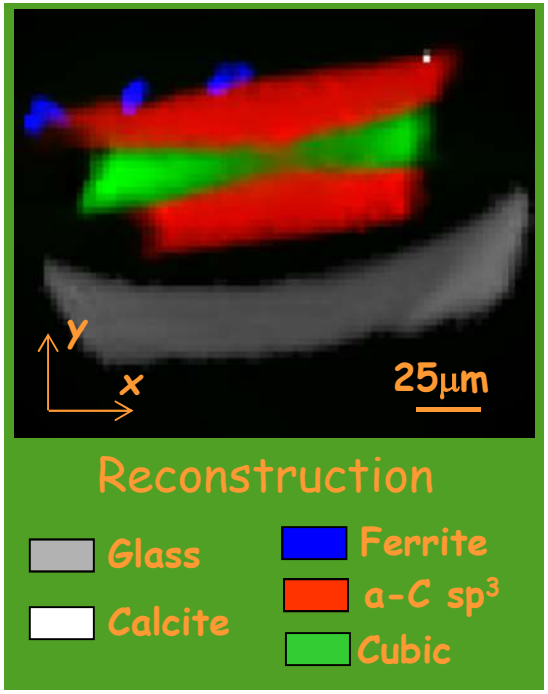

Bleuet et al., *Nature Materials* 2008

XRD-CT of mechanically modified ZrO ceramics

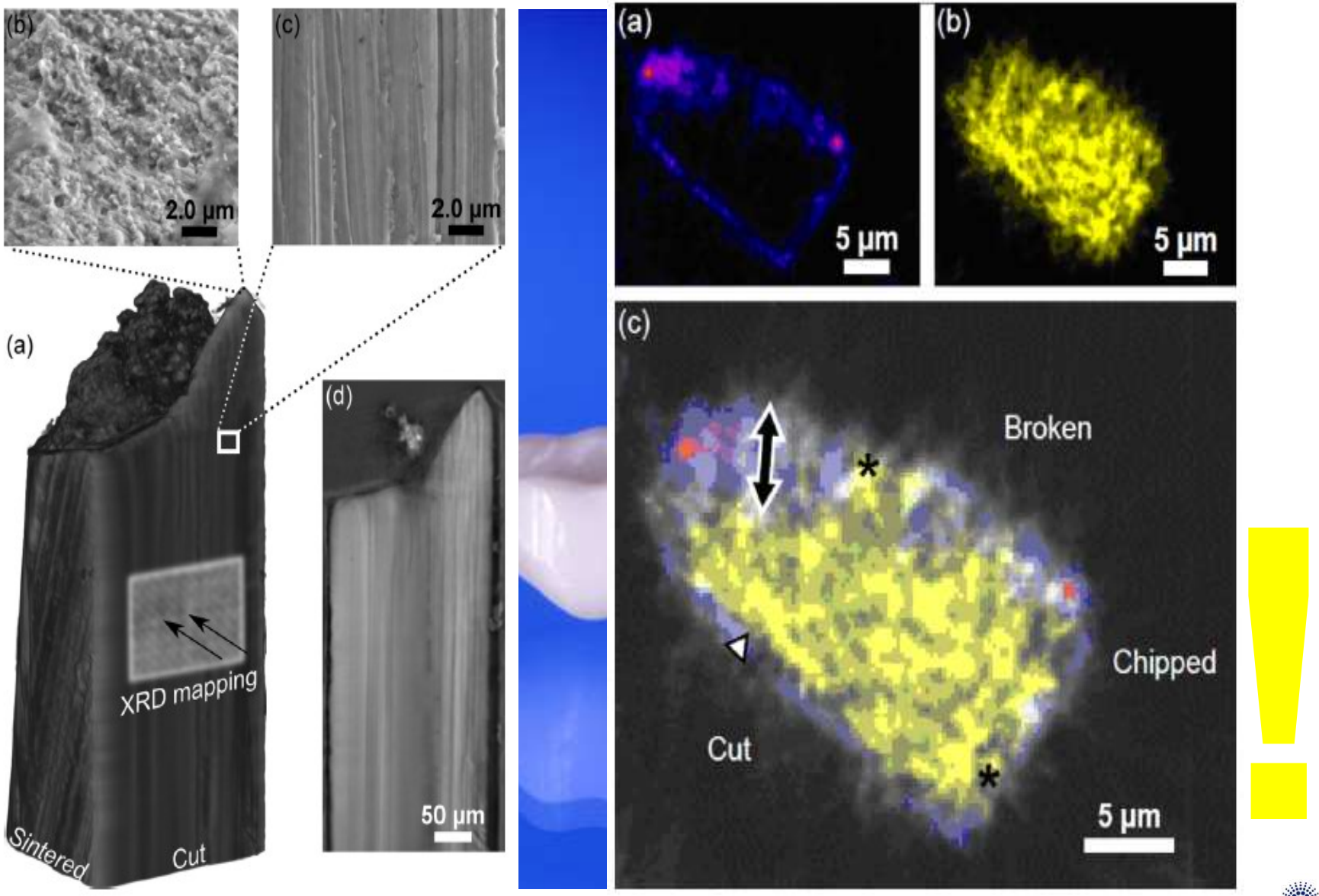

Time-resolved Microtomography

SOLIDIFICATION

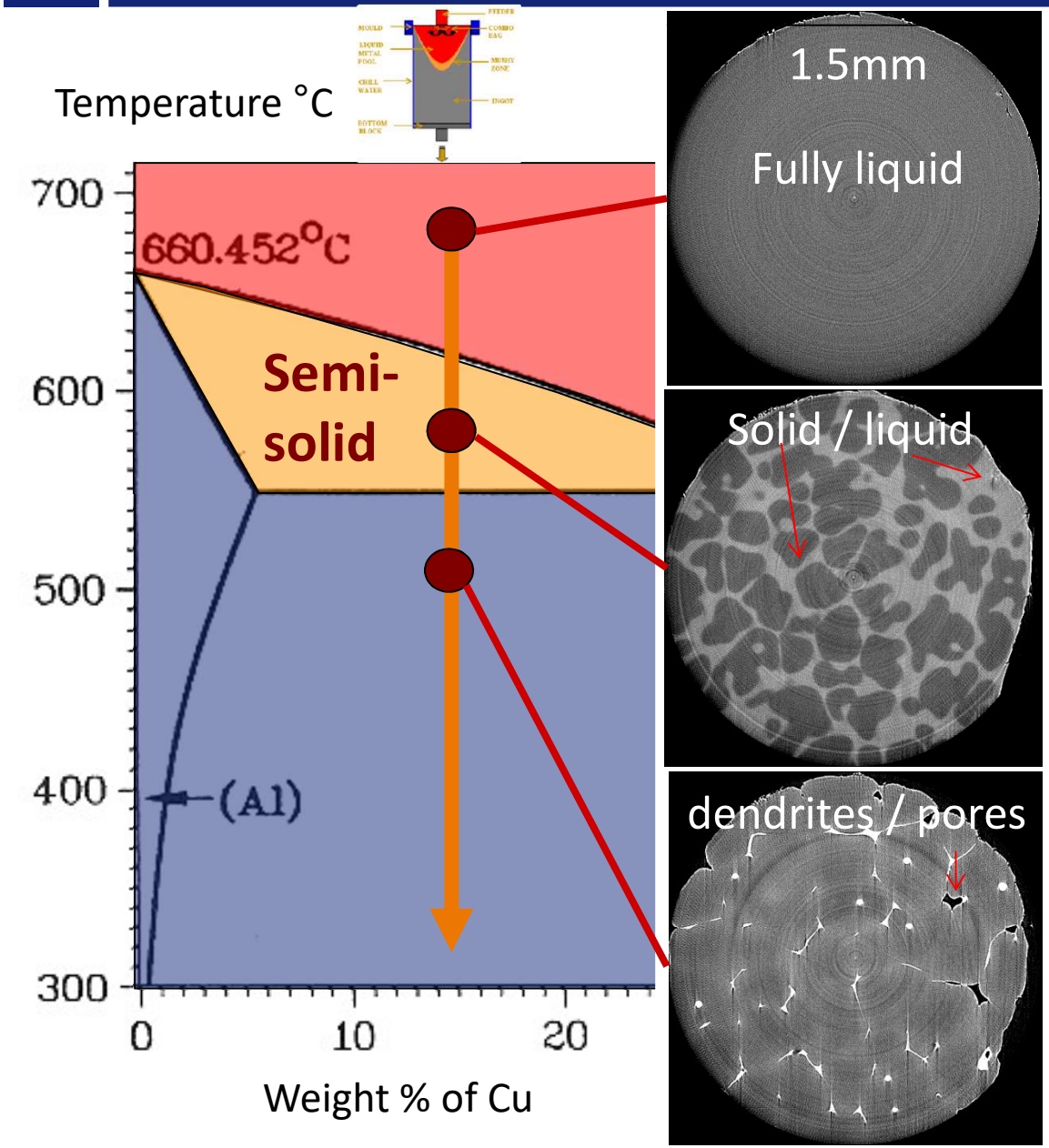

Solid fraction evolution
Solid coherency
Dendrite growth
Pore formation

Relevant scale
1µm –few µm

Typical cooling rates
0.1 – 10 °C/s

Courtesy Luc Salvo, CNRS

ULTRA-FAST RADIOSCOPY – LIQUID METAL FOAMS

Solidification Al 20% Cu
ID15A
PCO DIMAX, Size 780 x 600
600 projections, Optics 2.2µm
White beam (gap open)
Scan time 0.15 seconds
70 scans,

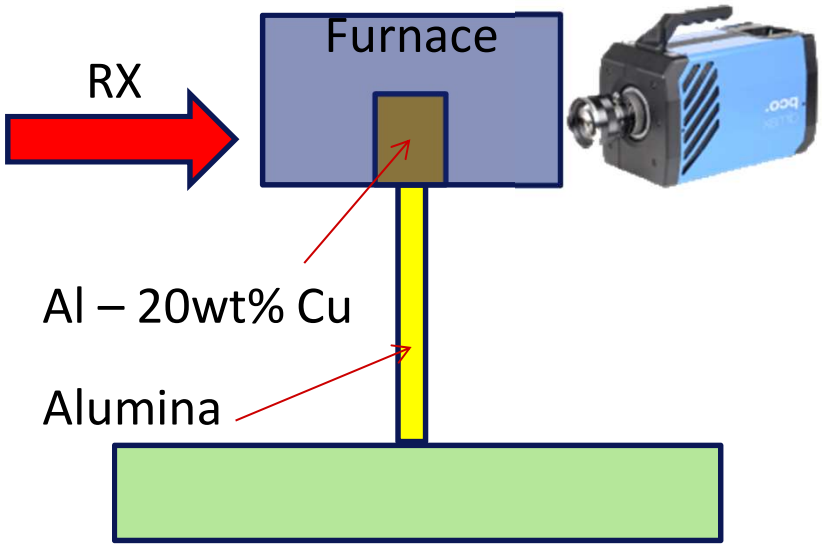

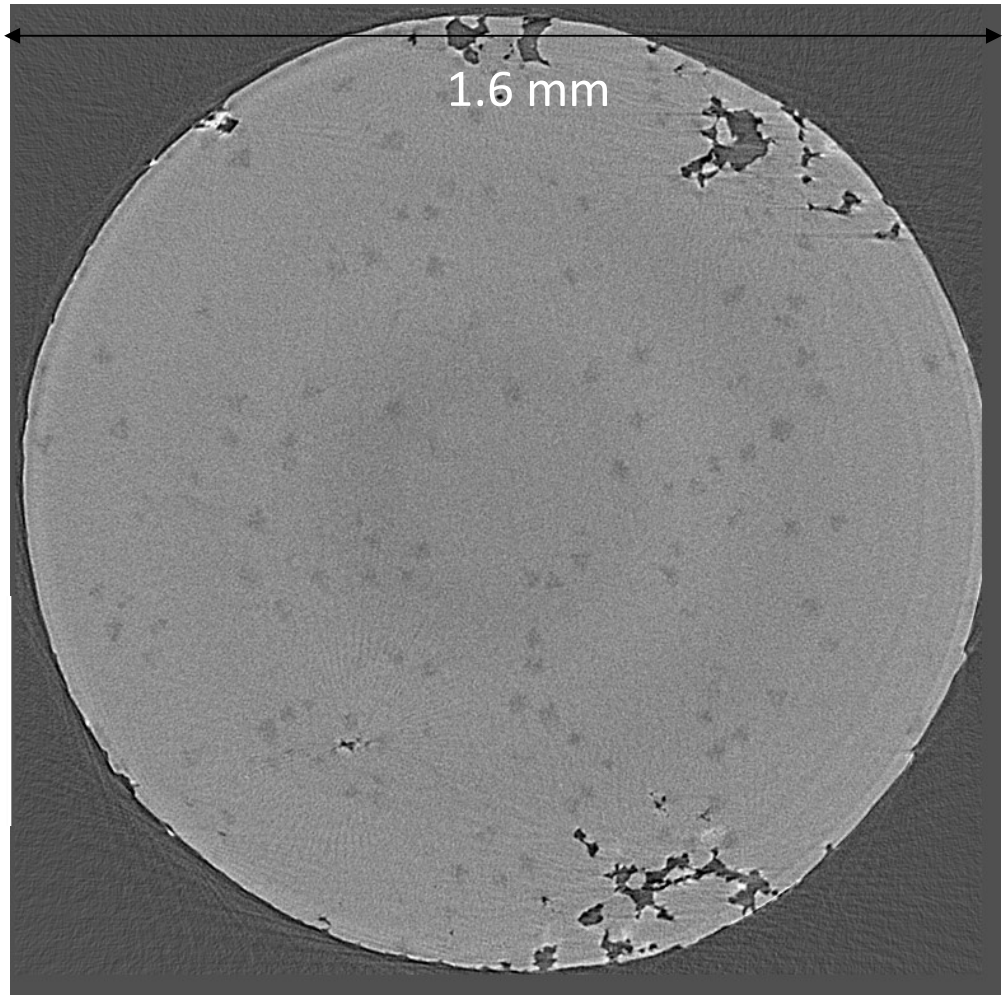

Solidification rate ~ 5°C/s
Solidification time 10s !!

Courtesy Luc Salvo, CNRS

IN-SITU GLASS MELTING: THE FATE OF CALCIUM CARBONATE PARTICLES

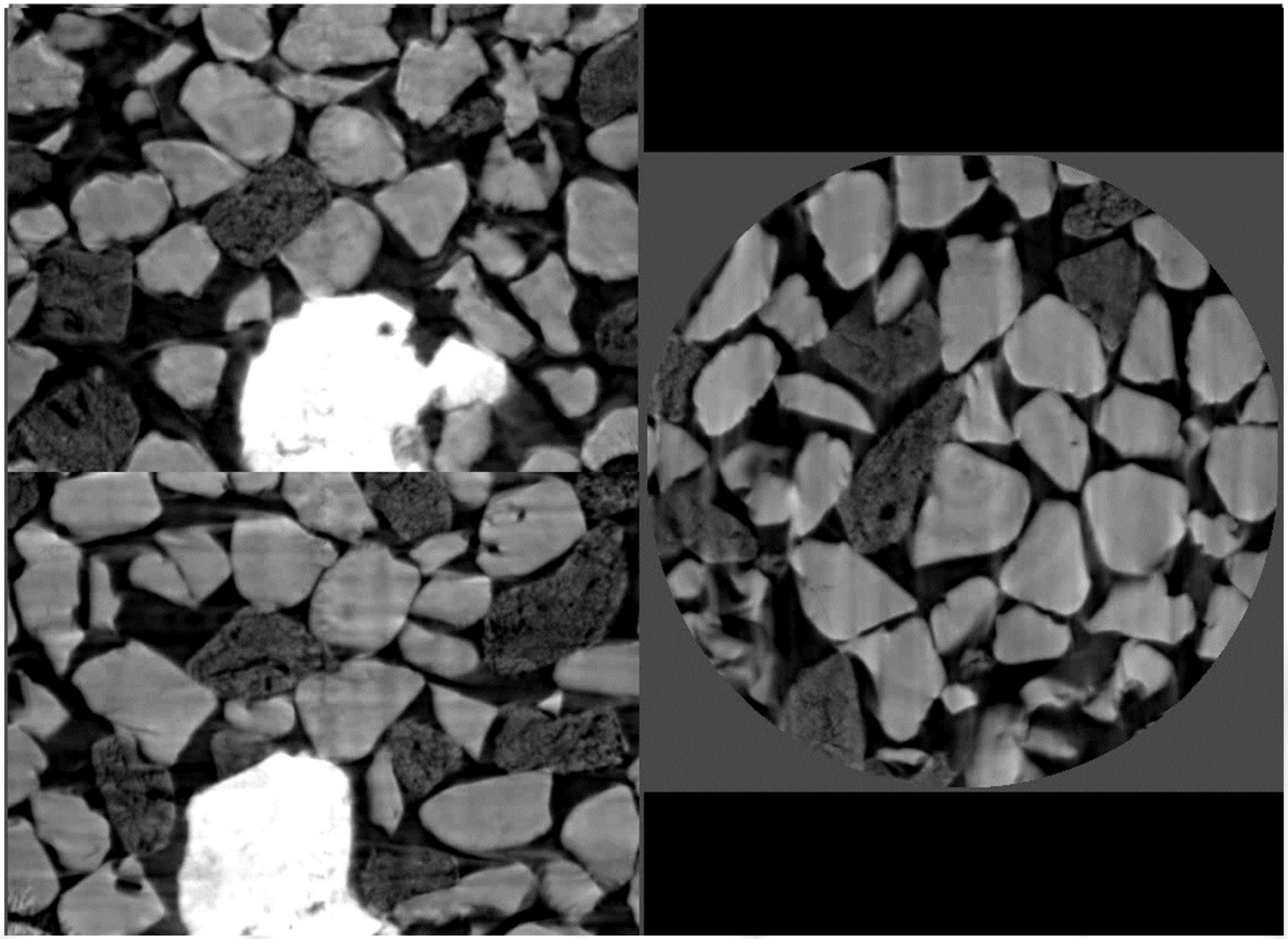

Fast heating at 900°C, ternary mixture of SiO_2, Na_2CO_3, $CaCO_3$

Courtesy E. Gouillart, St. Gobain

Ultimate Resolution in Time

ULTRA FAST ACQUISITION: SINGLE-BUNCH IMAGING

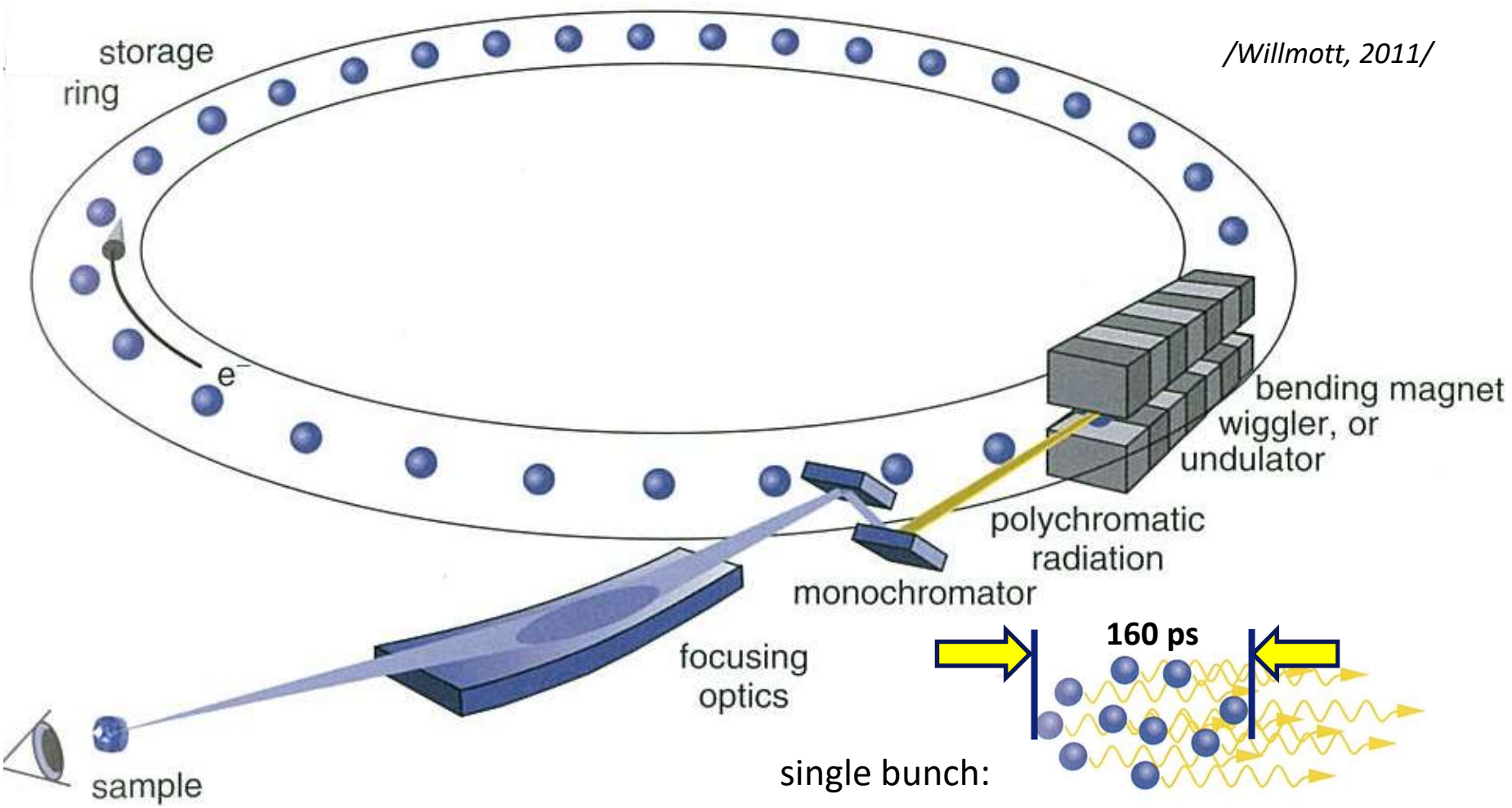

/Willmott, 2011/

- revolution 2.8 µs
- 4 bunches = 1.4 MHz frame rate
- Approx. 160 ps flash exposure

BUNCH IMAGING: MOVIE – LASER INDUCED BUBBLE COALESCENCE

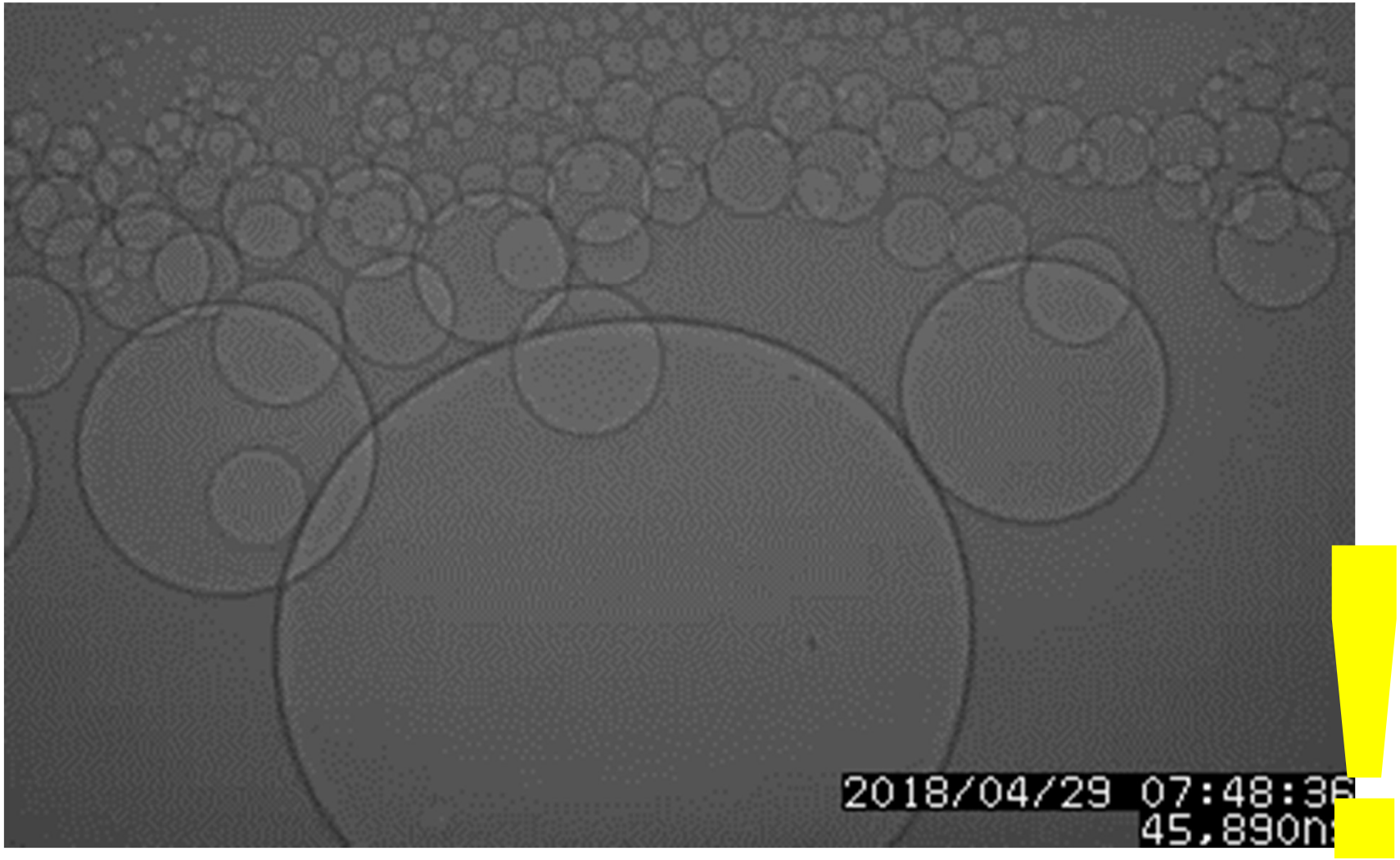

Rack, Olbinado – ID19 (unpublished data)

SINGLE-BUNCH RADIOSCOPY DEVELOPMENT: SHIMADZU HPV-X

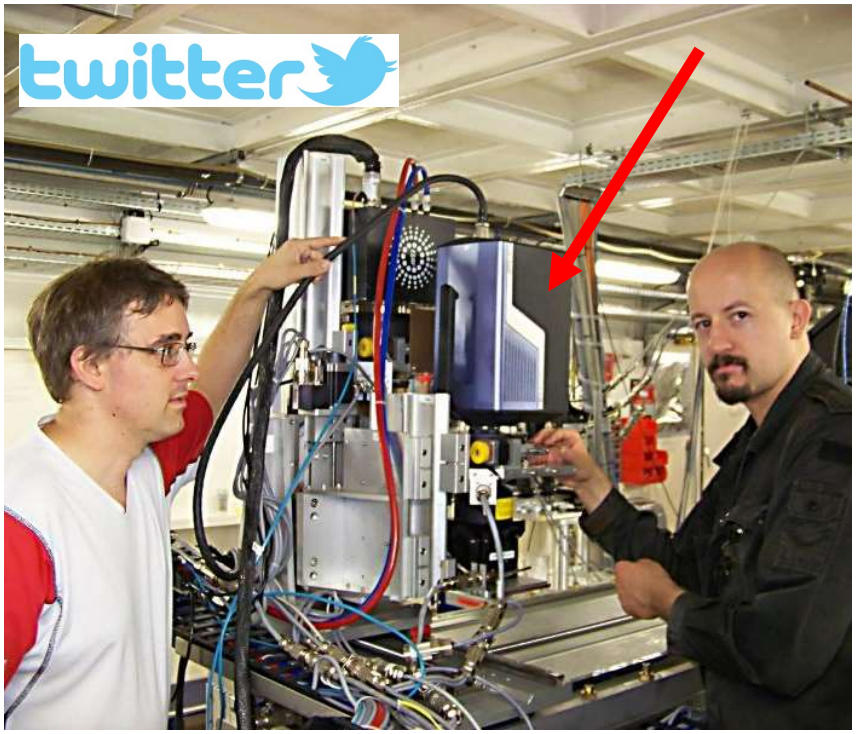

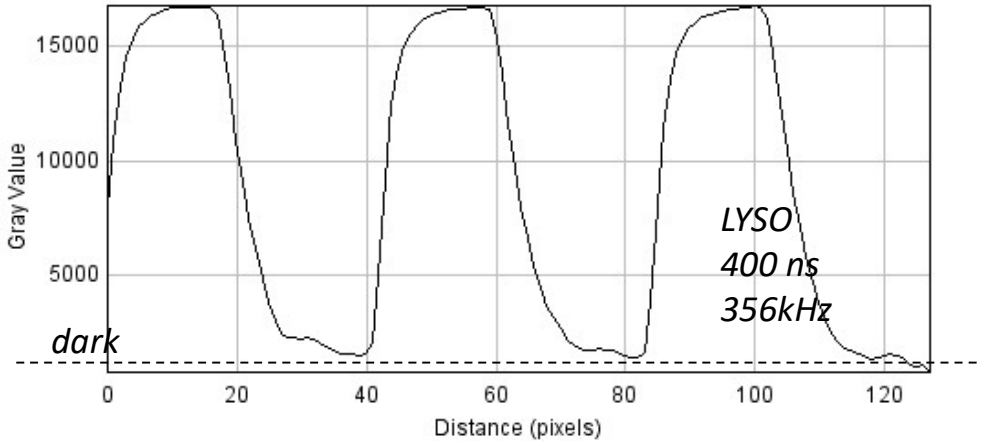

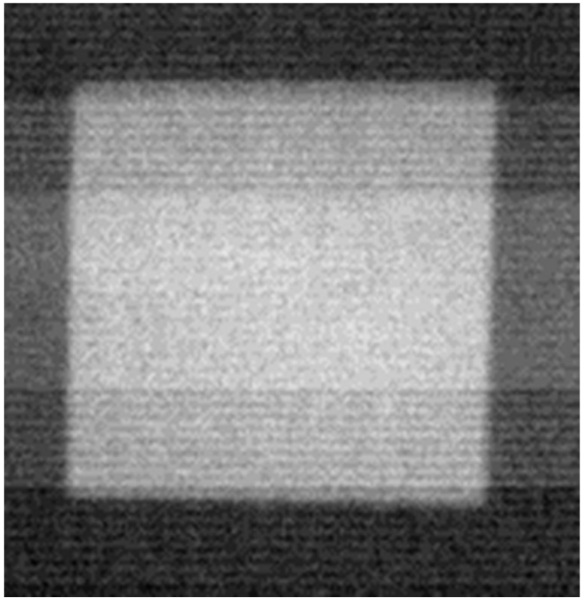

Shimadzu HPV-X2:

- 10 Mio images/second
- 128/256 ring buffer
- FrameTransfer CMOS (FTCMOS)

HIGH-SPEED ELECTRICAL FUSE BREAKING

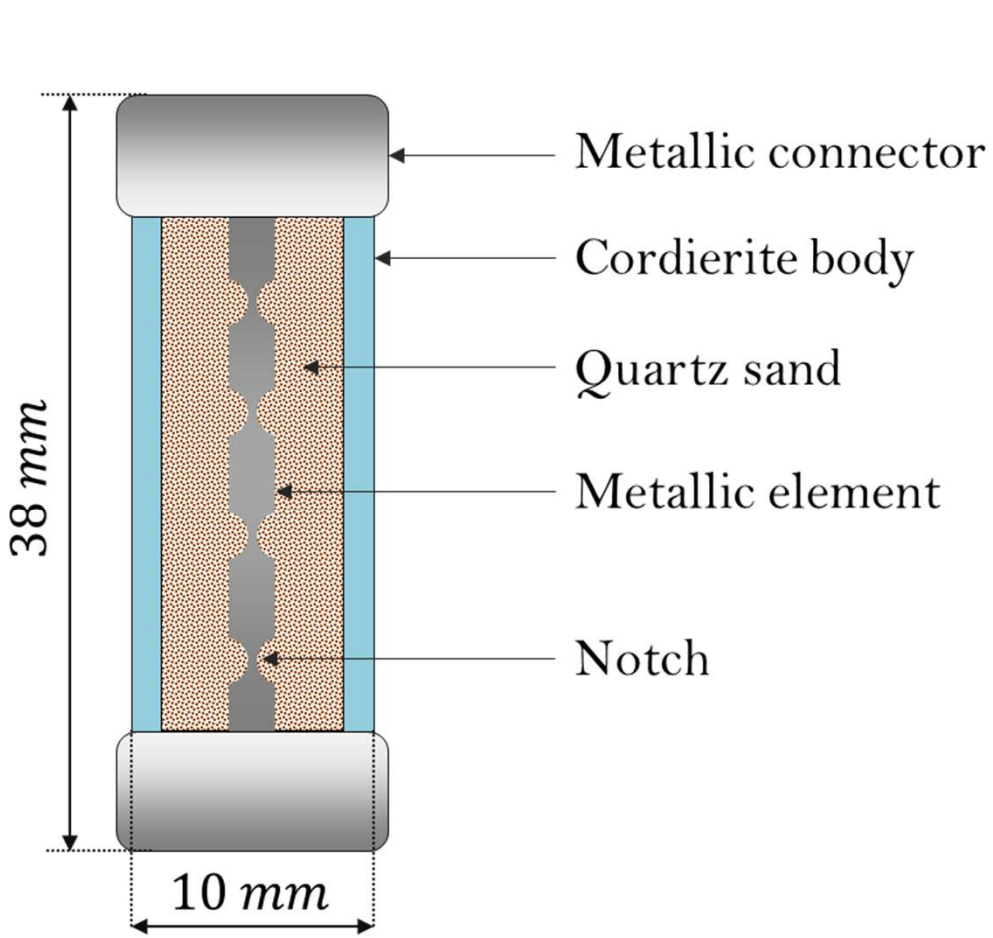

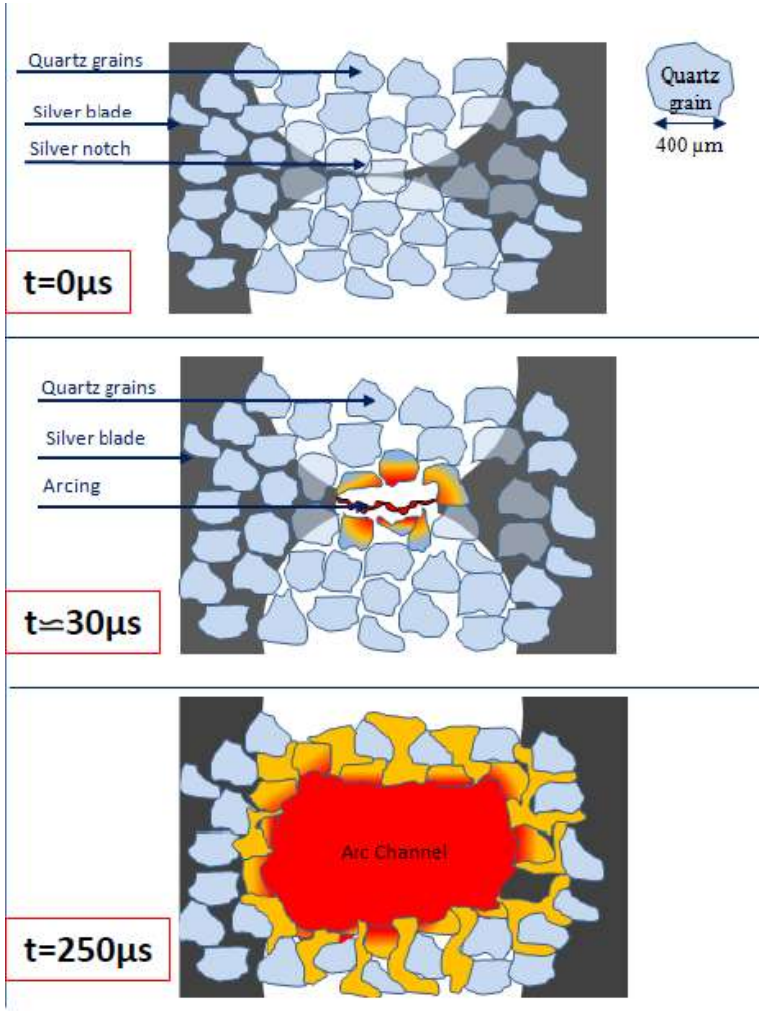

X. Just, P. Lhuissier, J.-M. Chaix (SIMAP), J.-L. Gelet, F. Balboni, M. Morati (Mersen)

MEGAFRAME-RATE RADIOSCOPY – FUSE with and w/o ENCAPSULATION

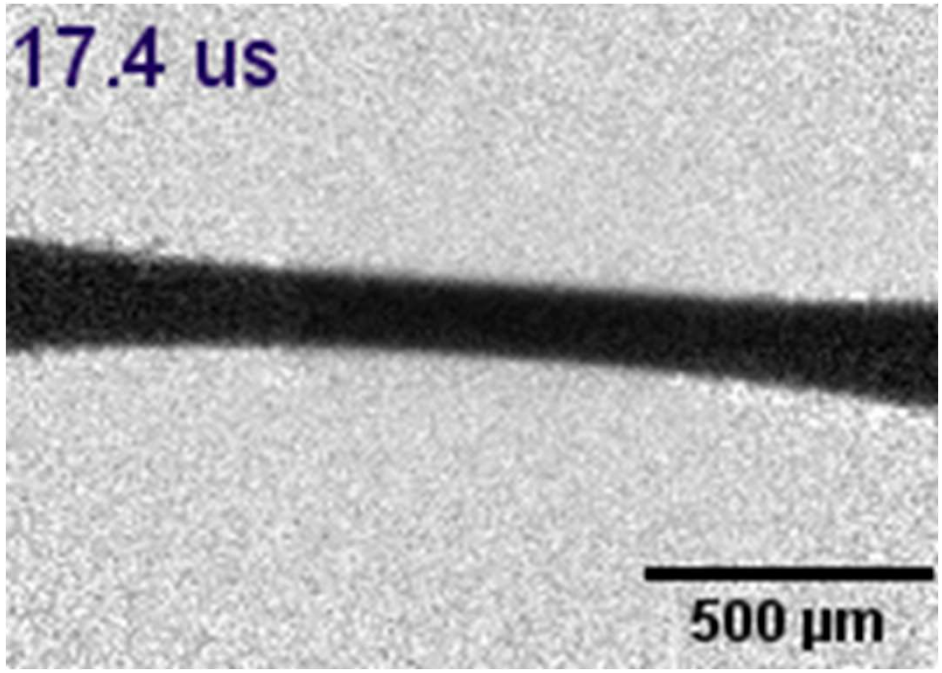

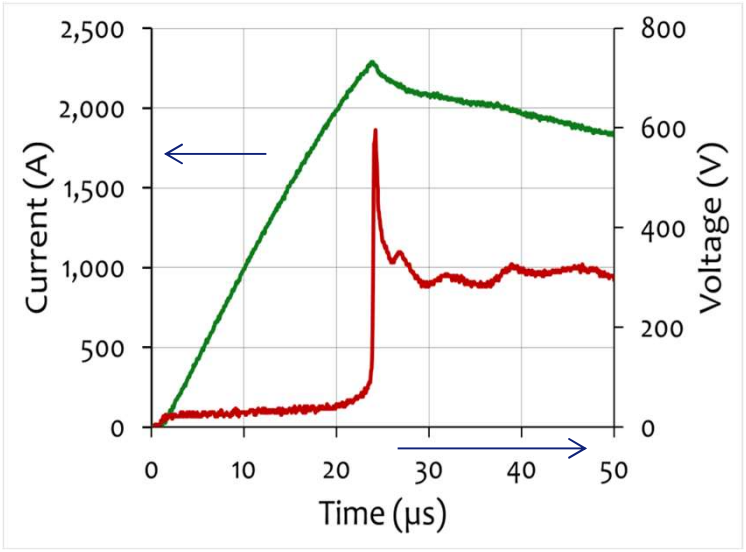

X. Just, P. Lhuissier, J.-M. Chaix (SIMAP), J.-L. Gelet, F. Balboni, M. Morati (Mersen)
A. Rack, M. Olbinado, E. Boller, J. Morse (ESRF)

IMPACT STUDIES WITH GAS GUN AND MHZ HARD X-RAY RADIOSCOPY

Eakins & Chapman,
RSI 85 (2014)

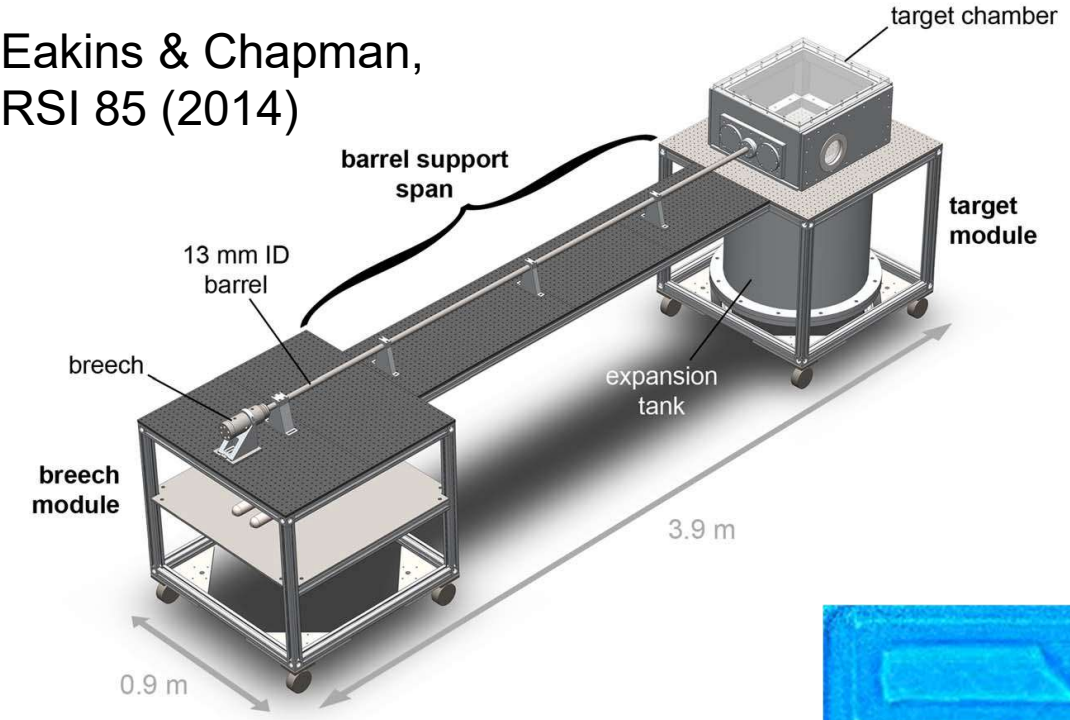

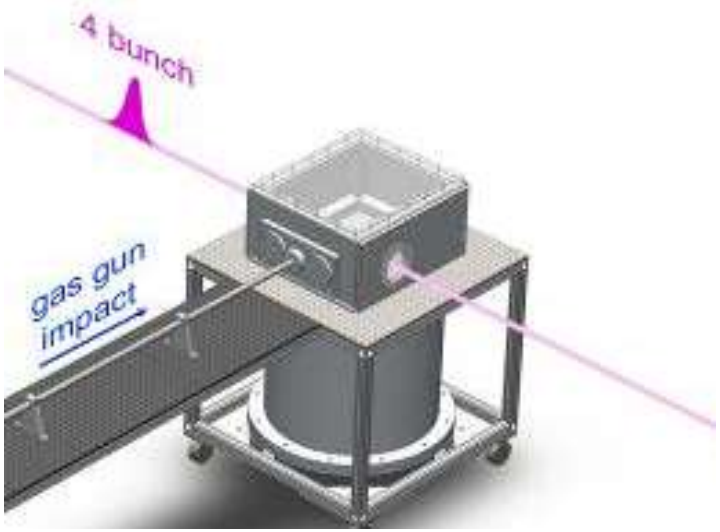

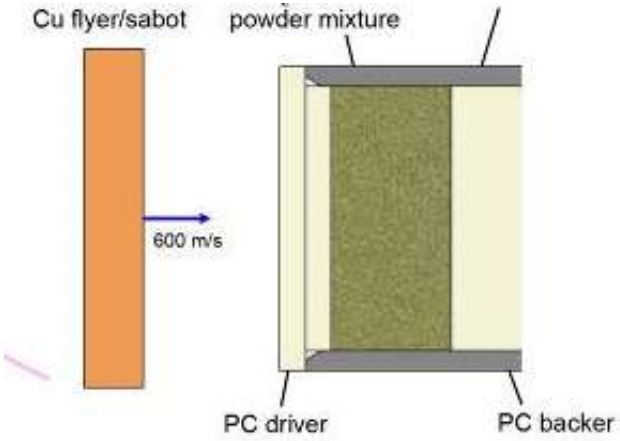

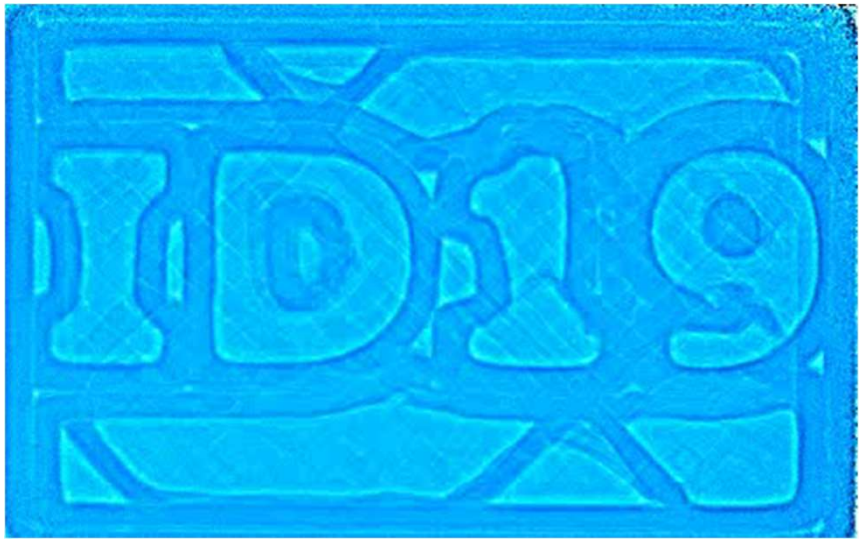

Oxford University, Imperial London

2-STAGE GAS GUN @ 3.8 MHz

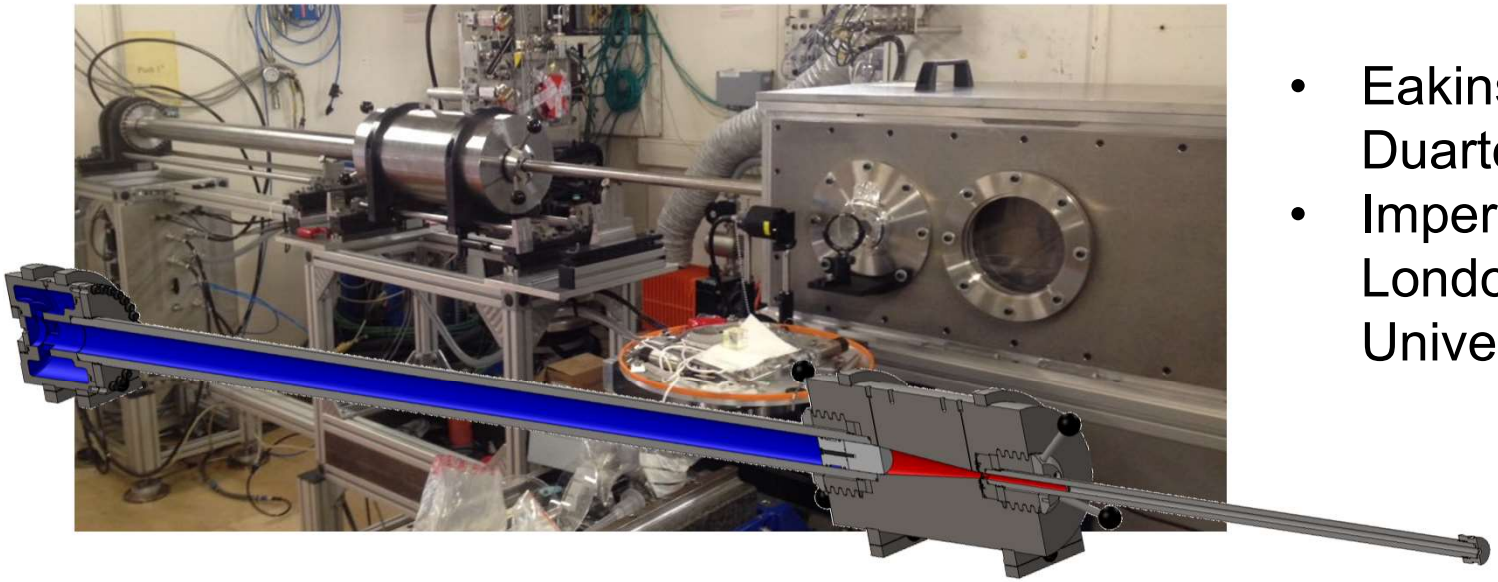

- Eakins, Chapman, Duarte et al.
- Imperial College London & Oxford University

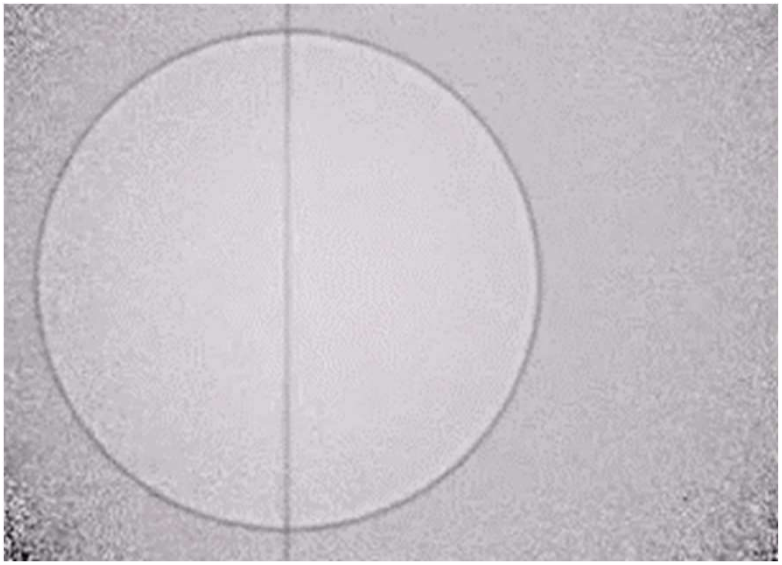

- two-stage launcher: impact 4 km/s
- 6 mm cavity; shockwave-driven collapse and jet formation
- velocity of the jet = ~2 x impact velocity; strength over-ridden, hydrodynamic flow regime
- video: 3.8 MHz = 2x 1.9 MHz
- Escauriza et al., Sci Rep 10 (2020)

PULSED-POWER-DRIVEN WIRE EXPLOSIONS IN WATER

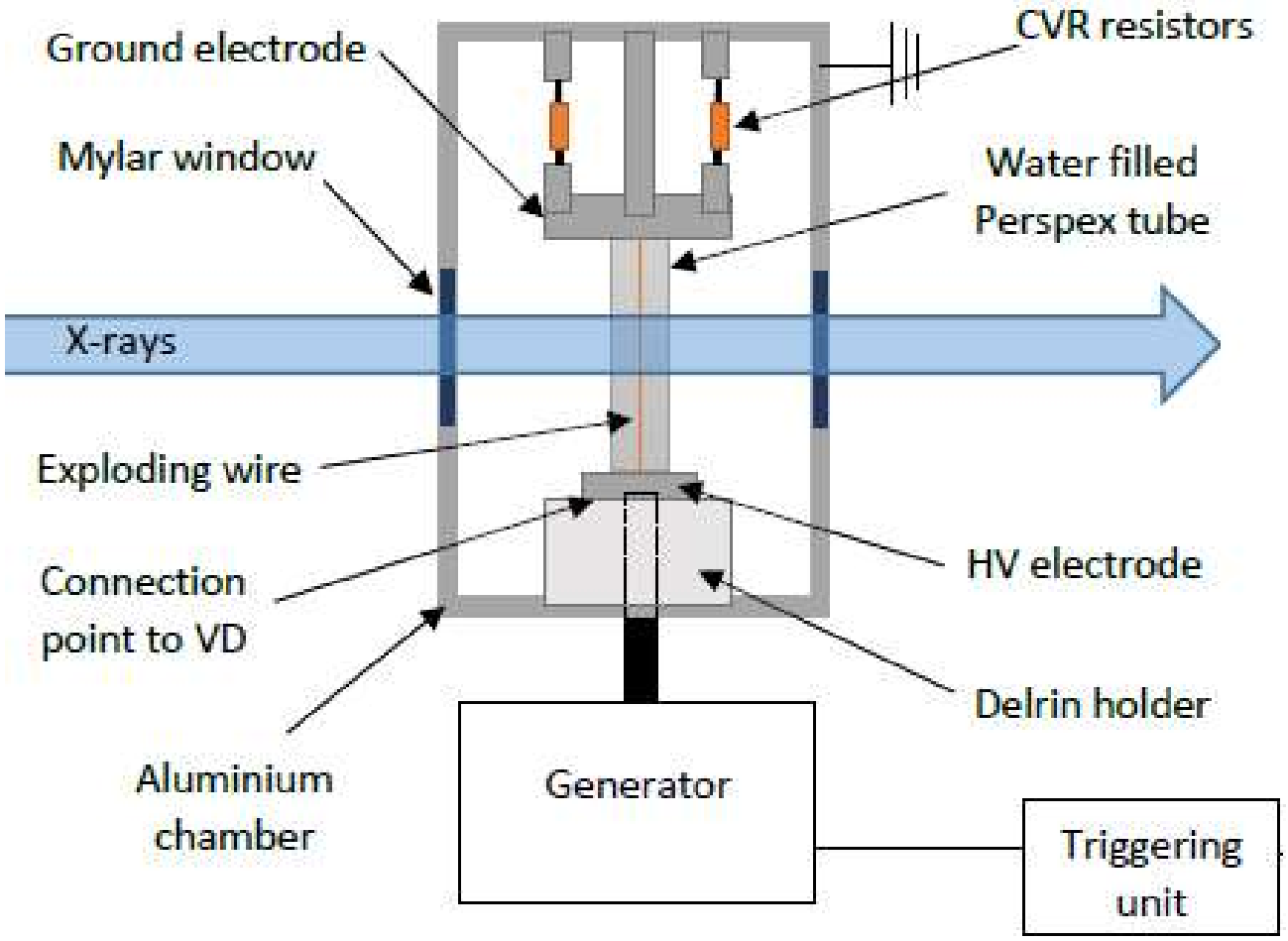

Imperial College London

In collaboration with S. Bland, D. Yanuka, A. Rasoshek, S. Theocharous, Y. E. Krasik (Imperial College London, UK)

D. Yanuka et al, J. Appl. Phys., vol. 124, 153301 (2018).
S. Theocharous, et al Rev. Sci. Instrum., vol. 90, 013504 (2019).
D. Yanuka et al, Physics of Plasma, submitted (2019).

PULSED-POWER-DRIVEN WIRE EXPLOSIONS IN WATER

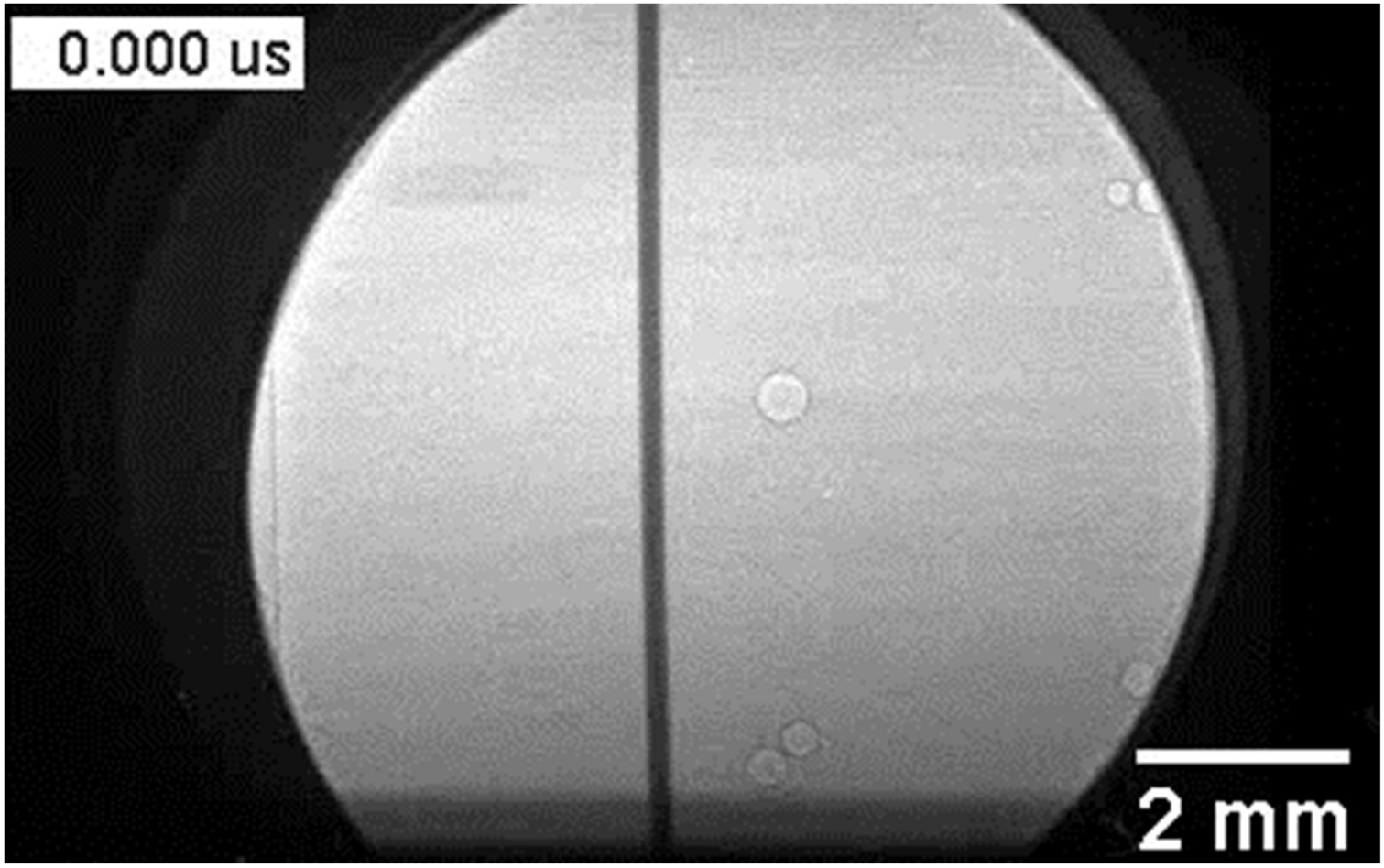

4-bunch filling mode (176 ns); polychromatic x-ray beam, mean 30 keV; 1.4 Mfps; exposure: 200 ns

Imperial College London

In collaboration with S. Bland, D. Yanuka, A. Rasoshek, S. Theocharous, Y. E. Krasik (Imperial College London, UK)

PULSED-POWER-DRIVEN WIRE EXPLOSIONS IN WATER

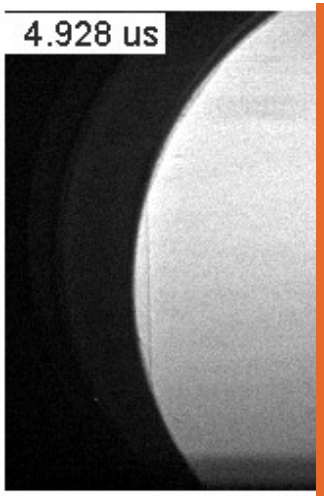

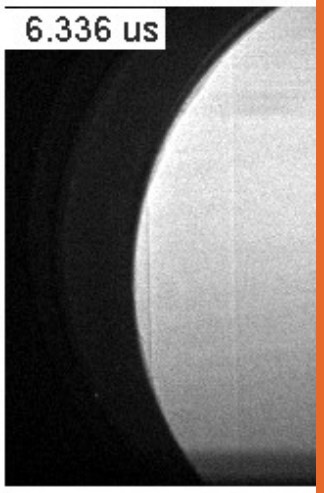

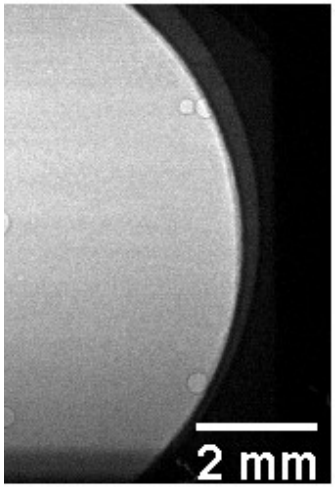

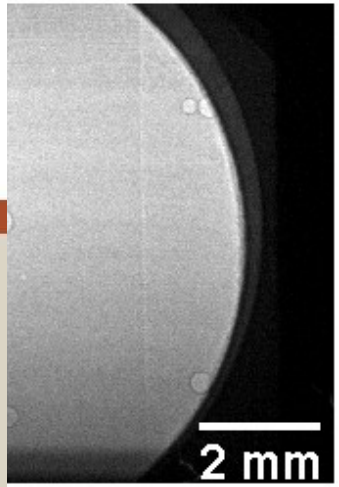

Journal of Applied Physics

AIP Publishing

scitation.org/journal/jap

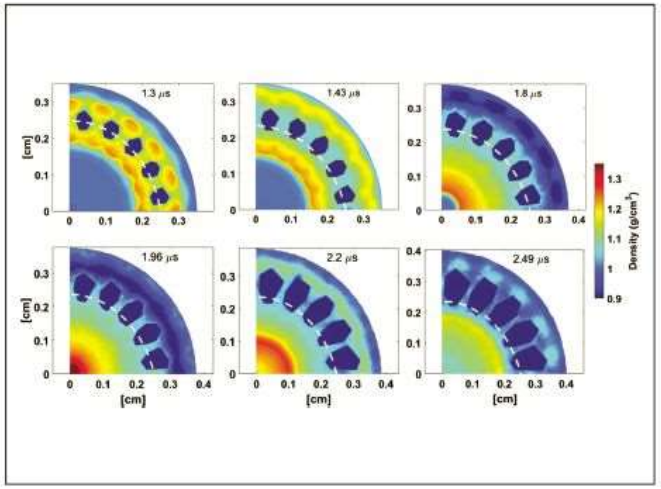

Volume 125, Issue 9, 7 Mar. 2019

Synchrotron based X-ray radiography of convergent shock waves driven by underwater electrical explosion of a cylindrical wire array

J. Appl. Phys. **125**, 017909 (2019); doi.org/10.1063/1.5089011

D. Yanuka, S. Theocharous, S. Efimov, S. N. Bland, *et al*

D. Yanuka et al, J. A

S. Theocharous, et

D. Yanuka et al, Phy

Imperial College London

LI-ION BATTERY THERMAL RUNAWAY

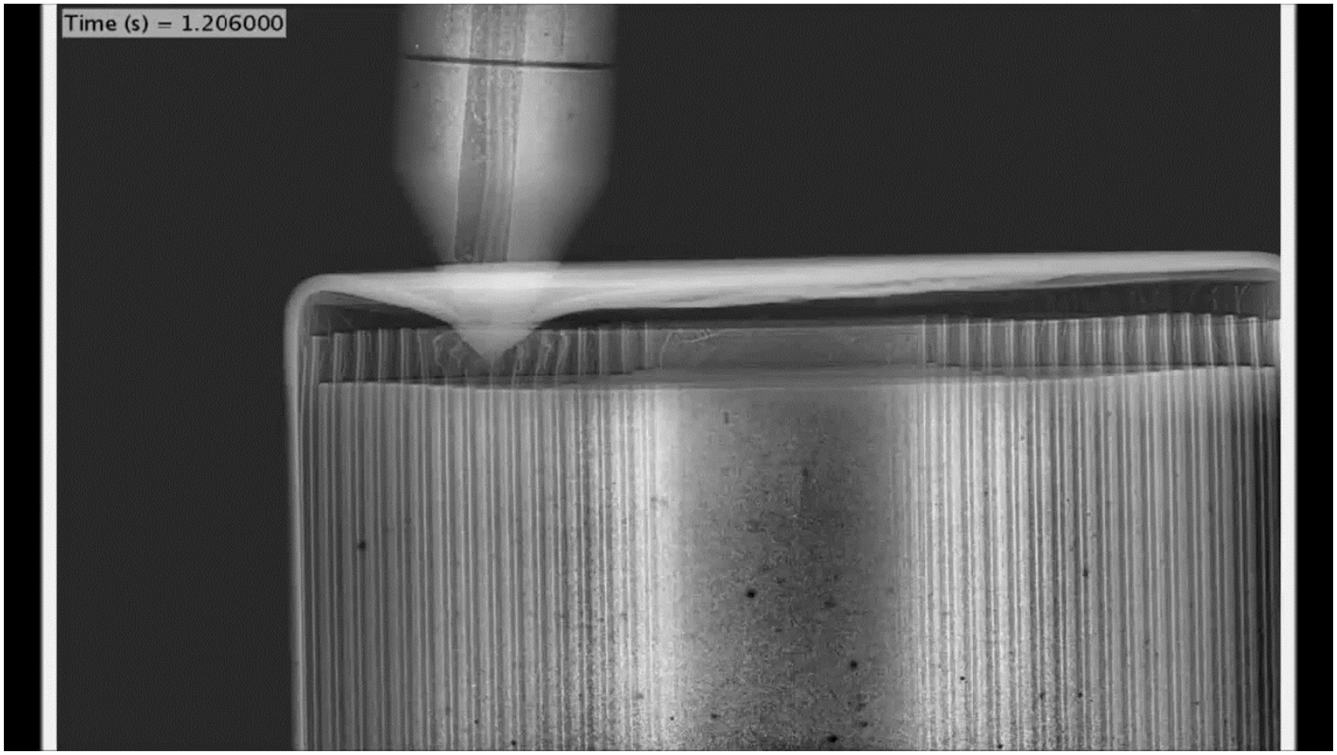

Polychromatic beam
Peak: 75 keV
pco. dimax, 1250 fps
LuAG: Ce

D. P. Finegan, et al, Identifying the cause of rupture of Li-ion batteries during thermal runaway Advanced Science, vol. 5, no. 1, 1700369 (2018)

Thank you for your attention!